

FIG. 8. Plot of the normalized square root of the measured area enclosed between the superconducting- and normal-state magnetization curves versus the square of the reduced temperature  $t = T/T_{c0}$ . These areas are for superconducting curves taken in increasing fields (see Fig. 3). For ideally reversible curves the ordinate is expected to be proportional to the "thermodynamic critical field"  $H_c$ . These results are thought to be consistent with the view that the  $H_c$  values are not appreciably altered by spin effects.

(3) The behavior of the magnetization of Ti-16 at. % Mo in the vicinity of the upper critical field suggests that the transition to the normal state is of second

order with a finite change in slope at the transition point. The change in slope is related to the electronic structure and the spin and spin-orbit effects by an expression which is a generalization due to Maki of Abrikosov's formula for the spin-independent case. The fair agreement between theory and experiment for the slope of the magnetization curve suggests that Abrikosov's vortex lattice solution may be an appropriate description of the magnetic structure even when spin effects are substantial.

#### ACKNOWLEDGMENTS

Special thanks are owed to D. H. Leslie for his excellent technical assistance in developing the apparatus and acquiring the data. I wish to thank K. Maki for the pre-publication use of his calculations, and finally I wish to acknowledge helpful discussions with T. G. Berlincourt at whose suggestion this study was undertaken.

### Strong-Coupling Superconductivity. I\*

D. J. SCALAPINO<sup>†</sup>, J. R. SCHRIEFFER, AND J. W. WILKINS<sup>‡</sup>

*Department of Physics, University of Pennsylvania, Philadelphia, Pennsylvania*

(Received 16 February 1966)

The pairing theory of superconductivity is extended to treat systems having strong electron-phonon coupling. In this regime the Landau quasiparticle approximation is invalid. In the theory we treat phonon and Coulomb interactions on the same basis and carry out the analysis using the nonzero-temperature Green's functions of the Nambu formalism. The generalized energy-gap equation thus obtained is solved (at  $T = 0^\circ\text{K}$ ) for a model which closely represents lead and the complex energy-gap parameter  $\Delta(\omega)$  is plotted as a function of energy for several choices of phonon and Coulomb interaction strengths. An expression for the single-particle tunneling density of states is derived, which, when combined with  $\Delta(\omega)$ , gives excellent agreement with experiment, if the phonon interaction strength is chosen to give the observed energy gap  $\Delta_0$  at zero temperature. The tunneling experiments therefore give a detailed justification of the phonon mechanism of superconductivity and of the validity of the strong-coupling theory. In addition, by combining theory and the tunneling experiments, much can be learned about the electron-phonon interaction and the phonon density of states. The theory is accurate to terms of order the square root of the electron-ion mass ratio,  $\sim 10^{-2}$ – $10^{-3}$ .

#### I. INTRODUCTION

IN the original BCS theory of superconductivity,<sup>1</sup> a central role was played by the concepts provided by Landau's theory of a Fermi liquid.<sup>2</sup> In Landau's theory,

\* This work was supported in part by the National Science Foundation and by the Laboratory for Research on the Structure of Matter, University of Pennsylvania, covering research sponsored by the Advanced Research Projects Agency. Part of the work reported here was performed as a portion of a thesis of one of us (J.W.W.) in partial fulfillment of the requirement for a Ph.D. degree in Physics, University of Illinois, 1963.

<sup>†</sup> Alfred P. Sloan Foundation Fellow.

<sup>‡</sup> Present address: Department of Physics, Cornell University, Ithaca, New York.

<sup>1</sup> J. Bardeen, L. N. Cooper, and J. R. Schrieffer, *Phys. Rev.* **108**, 1175 (1957).

<sup>2</sup> L. D. Landau, *Zh. Eksperim. i Teor. Fiz.* **30**, 1058 (1956).

the excited states  $\Phi_N$  of the Fermi liquid are placed in one-to-one correspondence with the excited states of a free Fermi gas. That is, the excited states  $\Phi_N$  are labelled by the occupation numbers  $\nu_{\mathbf{k}s}$  of the "quasi-particle" states of momentum  $\mathbf{k}$  and spin component  $s$  ( $\uparrow$  or  $\downarrow$ ) in analogy with single particle occupation numbers  $n_{\mathbf{k}s}$  of the free Fermi gas. Presumably the Landau configurations  $\Phi_N$  contain most of the many-body correlations occurring in the superconducting energy eigenfunctions  $\Psi_s$  except for those correlations which are specific to the superconducting phase, i.e., the pairing correlations.

Since the states  $\Phi_N$  form a complete set, a state  $\Psi_s$

of the super phase can be represented as a superposition

$$\psi_s = \sum_N C_N \Phi_N \quad (1.1)$$

of the Landau configurations. This representation has the attractive feature that in describing a given  $\Psi_s$  only a limited subset of all  $\Phi_N$ 's are required. This great simplification of the configuration interaction problem is due to two facts. Since the Landau configurations already contain the correlations present in the normal phase, the normal phase type correlations present in  $\Psi_s$  will not mix different  $\Phi_N$ 's. While the remaining pairing correlations do mix various  $\Phi_N$ 's, these states are restricted to a small subset by the pairing condition of the BCS theory. In simple cases, this condition corresponds to the requirement of correlated occupancy of time reversed states of the Landau theory (e.g.,  $\mathbf{k}\uparrow, -\mathbf{k}\downarrow$  for a translationally invariant system).

The above simplifications reduce the configuration interaction problem to a solvable form if one assumes the validity of the Landau theory and assumes a simple two-body interaction between Landau's quasiparticles. This simple but powerful scheme has led to a detailed understanding of the properties of most superconductors.<sup>3</sup>

There is, however, a class of superconductors such as Pb, Hg, etc., which cannot be treated by such a procedure. The difficulty can be seen in the following manner. In constructing a superconducting energy eigenfunction  $\Psi_s$ , the configurations  $\Phi_N$  which give the largest contribution to the pairing correlation energy are typically those in which quasiparticles are excited above the Fermi surface by an energy of order the average phonon energy [i.e.,  $\approx \hbar\omega_D$ , where  $\omega_D$  is the Debye frequency]. The average phonon energy enters here because the attractive interaction which causes superconductivity is due to virtual exchange of phonons, and this interaction is strongest when energy is nearly conserved during the emission or absorption of the virtual phonon.

Now the Landau theory works best when quasiparticles are excited to states  $\mathbf{k}$  in the immediate vicinity of the Fermi surface  $k_F$ . In this case an effective mass approximation for the quasiparticle energy  $\epsilon_{\mathbf{k}}$  can be used. [Note:  $\epsilon_{\mathbf{k}}=0$  for  $|\mathbf{k}|=k_F$ ; that is, quasiparticle energies are measured relative to the Fermi surface.] More important is the fact that the lifetime  $\tau_{\mathbf{k}}$  of these low-lying excited states is so long that the corresponding level width  $\Gamma_{\mathbf{k}}=\hbar/2\tau_{\mathbf{k}}$  can be neglected in comparison with  $\epsilon_{\mathbf{k}}$ . This is the approximation of the Landau theory. As one goes to higher energy quasiparticle states, the level widths of the states increases due to the increased rate for a quasiparticle to decay by emitting a phonon. An important question is then whether the lifetime of a quasiparticle of energy  $\epsilon_{\mathbf{k}}\approx\hbar\omega_D$  is so short that the level width of these states is of order the excitation

energy  $\epsilon_{\mathbf{k}}$ . If this is the case, as it is for strong-coupling superconductors, the Landau theory cannot be used as a basis for treating superconductivity in these metals. This is not to say that the Landau theory does not hold in the normal phase of these metals at temperatures small compared to the Debye temperature. Rather, the pairing interaction involves important virtually excited quasiparticle states which cannot be handled by the Landau theory (even at zero temperature). For weak-coupling superconductors, such as Al, Zn, etc., the quasiparticle lifetimes are sufficiently long that reasonably well-defined states exist even for  $\epsilon_{\mathbf{k}}\approx\hbar\omega_D$ . Therefore one can treat the weak-coupling superconductors from the point of view of the Landau theory, as in the BCS approach.

In addition to this problem of quasiparticle damping, one is faced with the problem of treating the retarded nature of the phonon interaction between electrons. This is a nontrivial problem even for weak coupling superconductors. As Eliashberg showed,<sup>4</sup> even in the weak-coupling limit the correct form of the retarded interaction which enters the energy-gap equation differs from those given by Fröhlich,<sup>5</sup> by Bardeen and Pines,<sup>6</sup> and by Bogoliubov.<sup>7</sup>

Viewed as a field-theoretical problem, it might appear that one has little hope of handling this strongly coupled fermion-boson system in an accurate manner. The reason that one can give an essentially exact treatment of the problem follows from an important discovery of Migdal<sup>8</sup> in his treatment of the coupled electron-phonon system in normal metals. He showed that in normal metals one can calculate the one-electron self-energy to an accuracy of order  $(m/M)^{1/2}$  ( $m\equiv$  electronic mass,  $M\equiv$  ionic mass)  $\sim 10^{-2}$  by what amounts to second-order self-consistent perturbation theory. This remarkable result does not depend upon the strength of the electron-phonon coupling but rather depends on the existence of the small parameter  $(m/M)^{1/2}$  in the problem. The generalization of Migdal's result to superconducting metals was given by Eliashberg<sup>4</sup> and by Nambu.<sup>9</sup>

In this paper we generalize the Eliashberg-Nambu scheme by taking account of the Coulomb as well as the phonon interactions between electrons.<sup>10</sup> Equations

<sup>4</sup> G. M. Eliashberg, Zh. Eksperim. i Teor. Fiz. 38, 966 (1960) [English transl.: Soviet Phys.—JETP 11, 696 (1960)].

<sup>5</sup> H. Fröhlich, Phys. Rev. 79, 845 (1950).

<sup>6</sup> J. Bardeen and D. Pines, Phys. Rev. 99, 1140 (1955).

<sup>7</sup> N. N. Bogoliubov, Zh. Eksperim. i Teor. Fiz. 34, 58 (1958) [English transl.: Soviet Phys.—JETP 7, 41 (1958)].

<sup>8</sup> A. B. Migdal, Zh. Eksperim. i Teor. Fiz. 34, 1438 (1958) [English transl.: Soviet Phys.—JETP 7, 996 (1958)].

<sup>9</sup> Y. Nambu, Phys. Rev. 117, 648 (1960).

<sup>10</sup> Using a similar "realistic" interaction, P. Morel and P. W. Anderson have given an approximate solution for the pairing part of the self-energy [Phys. Rev. 125, 1263 (1962)]. A numerical solution for the pairing self-energy was reported by G. J. Culler, B. C. Fried, R. W. Huff, and J. R. Schrieffer, Phys. Rev. Letters 8, 399 (1962). In both these calculations the "normal" part of the self-energy which is important for strong-coupling superconductors was neglected.

<sup>3</sup> J. Bardeen and J. R. Schrieffer, *Progress in Low Temperature Physics* (North-Holland Publishing Company, Amsterdam, 1961), Vol. III.

determining the electronic self-energy as a function of temperature are derived in Sec. II. In Sec. III an expression for the effective tunneling density of states is determined. This density of states depends upon the complex, frequency-dependent gap part of the electronic self-energy. In Sec. IV the parameters of the model used for Pb are discussed and the solutions of the self-energy equations presented. Using these solutions, the effective tunneling density of states is calculated and compared to the experimental tunneling data.<sup>11</sup> The results show that tunneling measurements provide a delicate probe of the structure of the electronic self-energy and reflect the properties of the underlying effective electron-electron interaction.

## II. SELF-ENERGY EQUATIONS

### A. Structure of the Equations

To treat strong coupling superconductors, we use the formalism of Nambu.<sup>9</sup> In this scheme one introduces a two-component electron field operator

$$\Psi_{\mathbf{p}} = \begin{pmatrix} c_{\mathbf{p}\uparrow} \\ c_{-\mathbf{p}\downarrow}^\dagger \end{pmatrix} \quad (2.1a)$$

whose components  $c_{\mathbf{p}\uparrow}$  and  $c_{-\mathbf{p}\downarrow}^\dagger$  destroy an electron in a Bloch state of crystal momentum  $\mathbf{p}$  and spin orientation  $\uparrow$ , and create an electron in the time reversed state  $-\mathbf{p}\downarrow$ , respectively. The bare-phonon field operator

$$\varphi_{\mathbf{q}\lambda} = a_{\mathbf{q}\lambda} + a_{-\mathbf{q}\lambda}^\dagger \quad (2.1b)$$

is a linear combination of a destruction and a creation operator for bare phonons of mode  $\lambda$  and wave vector  $\mathbf{q}$  and  $-\mathbf{q}$ , respectively. The Hamiltonian of the system can be expressed in terms of  $\Psi_{\mathbf{p}}$  and  $\varphi_{\mathbf{q}\lambda}$  as

$$\begin{aligned} H = & \sum_{\mathbf{p}} \epsilon_{\mathbf{p}} \Psi_{\mathbf{p}}^\dagger \tau_3 \Psi_{\mathbf{p}} + \sum_{\mathbf{q}\lambda} \Omega_{\mathbf{q}\lambda} a_{\mathbf{q}\lambda}^\dagger a_{\mathbf{q}\lambda} \\ & + \sum_{\mathbf{p}\mathbf{p}'\lambda} g_{\mathbf{p}\mathbf{p}'\lambda} \varphi_{\mathbf{p}-\mathbf{p}'\lambda} \Psi_{\mathbf{p}'\uparrow}^\dagger \tau_3 \Psi_{\mathbf{p}} \\ & + \frac{1}{2} \sum_{\mathbf{p}_1\mathbf{p}_2\mathbf{p}_3\mathbf{p}_4} \langle \mathbf{p}_3\mathbf{p}_4 | V_c | \mathbf{p}_1\mathbf{p}_2 \rangle (\Psi_{\mathbf{p}_3}^\dagger \tau_3 \Psi_{\mathbf{p}_1}) \\ & \quad \times (\Psi_{\mathbf{p}_4}^\dagger \tau_3 \Psi_{\mathbf{p}_2}) + \text{const.} \quad (2.2) \end{aligned}$$

Here  $\epsilon_{\mathbf{p}}$  is the Bloch energy measured relative to the Fermi energy  $E_F$ , and  $\tau_1$ ,  $\tau_2$  and  $\tau_3$  are the Pauli matrices. We work in units with  $\hbar=1$ . The quantities  $\Omega$ ,  $g$  and  $V_c$  represent the bare phonon frequencies, the bare electron-phonon coupling, and the bare Coulomb interaction between electrons respectively. Translational invariance of  $V_c$  restricts  $\mathbf{p}_1+\mathbf{p}_2-\mathbf{p}_3-\mathbf{p}_4$  to be zero or a reciprocal lattice vector  $\mathbf{K}$ . We work in a box of unit volume and impose periodic boundary conditions. The electrons are described in an extended zone scheme and the phonons described in a reduced zone

<sup>11</sup> We have previously reported some of these results, J. R. Schrieffer, D. J. Scalapino, and J. W. Wilkins, Phys. Rev. Letters **10**, 336 (1963).

scheme which is formally extended periodically throughout  $q$  space to allow umklapp processes to be handled automatically.

Since we are ultimately interested in deriving expressions for the thermodynamic and transport properties of superconductors, we concentrate on calculating the Green's functions which determine these quantities. The one-particle thermodynamic Green's functions are defined in the Nambu scheme to be

$$G(\mathbf{p}, \tau) = -\langle UT \{ \Psi_{\mathbf{p}}(\tau) \Psi_{\mathbf{p}}^\dagger(0) \} \rangle, \quad (2.3a)$$

$$D_\lambda(\mathbf{q}, \tau) = -\langle T \{ \varphi_{\mathbf{q}\lambda}(\tau) \varphi_{\mathbf{q}\lambda}^\dagger(0) \} \rangle, \quad (2.3b)$$

where the average is taken in the grand canonical ensemble

$$\langle A \rangle \equiv \text{Tr}(e^{-\beta H} A) / \text{Tr} e^{-\beta H}.$$

The operators in (2.3) evolve with the "imaginary time"  $i\tau$  according to

$$\Psi_{\mathbf{p}}(\tau) = e^{H\tau} \Psi_{\mathbf{p}}(0) e^{-H\tau}, \quad (2.3c)$$

$$\varphi_{\mathbf{q}\lambda}(\tau) = e^{H\tau} \varphi_{\mathbf{q}\lambda}(0) e^{-H\tau}. \quad (2.3d)$$

The symbol  $T$  represents the conventional  $\tau$ -ordered product and the operator  $U$  in (2.3a) is given by

$$U = 1 + R^\dagger + R,$$

where  $R^\dagger$  converts a given state in an  $N$ -particle system into the corresponding state in the  $N+2$  particle system; thus for the ground states

$$R^\dagger |0, N\rangle = |0, N+2\rangle, \quad (2.4a)$$

$$R |0, N\rangle = |0, N-2\rangle, \quad (2.4b)$$

etc. Notice that  $G$  is a  $2 \times 2$  matrix, whose diagonal components  $G_{11}$  and  $G_{22}$  are the conventional Green's functions for up-spin electrons and down-spin holes, respectively, while  $G_{12}$  and  $G_{21}$  are Gorkov's<sup>12</sup>  $F$  and  $F^*$  functions which describe the pairing condensation. Due to the periodicity of  $G$  and  $D$  with respect to  $\tau$ , these functions can be represented by the Fourier series

$$G(\mathbf{p}, \tau) = 1/\beta \sum_{n=-\infty}^{\infty} e^{-i\omega_n \tau} G(\mathbf{p}, i\omega_n), \quad (2.5a)$$

$$D_\lambda(\mathbf{q}, \tau) = 1/\beta \sum_{n=-\infty}^{\infty} e^{-i\nu_n \tau} D_\lambda(\mathbf{q}, i\nu_n), \quad (2.5b)$$

where

$$\omega_n = (2n+1)\pi/\beta, \quad \nu_n = 2n\pi/\beta, \quad (2.5c)$$

$n$  being an integer.

The one-electron Green's function for the noninteracting system is easily seen to be given by

$$G_0(\mathbf{p}, i\omega_n) = [i\omega_n - \epsilon_{\mathbf{p}} \tau_3]^{-1}. \quad (2.6)$$

The electronic self-energy  $\Sigma(\mathbf{p}, i\omega_n)$  (a  $2 \times 2$  matrix) is

<sup>12</sup> L. P. Gorkov, Zh. Eksperim. i Teor. Fiz. **34**, 735 (1958) [English transl.: Soviet Phys.—JETP **7**, 505 (1958)].

then defined by Dyson's equation

$$[G(\mathbf{p}, i\omega_n)]^{-1} = [G_0(\mathbf{p}, i\omega_n)]^{-1} - \Sigma(\mathbf{p}, i\omega_n). \quad (2.7)$$

An important feature of the Nambu formalism is that the familiar Feynman-Dyson perturbation series rules (and their finite-temperature generalization) hold in calculating the  $G$  and  $D$ .

Our procedure is to set up an integral equation for  $\Sigma(\mathbf{p}, i\omega_n)$  which treats the electron-phonon interaction accurately to order  $(m/M)^{1/2} \sim s/v_F \sim \omega_D/E_F$ , where  $m/M$  is the electron-ion mass ratio,  $s/v_F$  is the ratio of speed of sound and the Fermi velocity, and  $\omega_D/E_F$  is the ratio of the Debye energy and the Fermi-energy. That such an integral equation can be found in closed form was shown for normal metals by Migdal<sup>8</sup> and for superconductors by Eliashberg.<sup>4</sup> In their analysis the theory was worked out at zero temperature and the Coulomb interaction  $V_c$  was neglected. Thus they took  $\Omega$  and  $g$  to be the appropriately screened quantities as in the Fröhlich model of the coupled electron-phonon system. Since the Coulomb interaction plays an important role in a consistent theory of superconductivity, we work with the Hamiltonian (2.2) rather than that used by Migdal and Eliashberg and carry out the analysis at finite temperature.

In setting up an integral equation for  $\Sigma$  it is important to note that we are mainly interested in physical excitations of energy  $\sim \omega_D \ll E_F$ . Higher energy states are not thermodynamically populated at superconducting temperatures. In addition, electron tunneling, electromagnetic absorption studies, etc. yield interesting information about the *superconducting* state primarily in this low-energy domain. Thus we are interested in the structure of  $\Sigma(\mathbf{p}, i\omega_n)$  for  $p \sim p_F$  and  $|\omega_n| \ll E_F$ . In this range the Coulomb interaction leads to important screening and renormalization effects, however it does *not* lead to interesting variations of  $\Sigma$  in a region  $\sim \omega_D$  about the Fermi surface as is evident on dimensional grounds. Thus, for our purposes the Coulomb interaction serves mainly to renormalize the bare electron and phonon-energy spectra and screen the electron-phonon interaction, as assumed in the Fröhlich model. In addition there remains a short range (screened) Coulomb repulsion which opposes superconductivity. As we will see, this short range (almost instantaneous) interaction must be handled in a manner different from that used for the (strongly retarded) phonon interaction between electrons.



FIG. 1. Electron self-energy diagrams for the screened Coulomb (dashed line) and dressed phonon (wavy line) exchange by the self-consistently dressed electron propagator (solid line).

Our basic approximation for  $\Sigma(\mathbf{p}, i\omega_n)$  is shown schematically in Fig. 1. The solid line represents  $G$  as given by Dyson's equation (2.7) in terms of this self-consistently determined self-energy. In the first diagram of this figure, the dashed line represents the electronically screened Coulomb interaction. If the Bloch functions were approximated by plane waves, the screened Coulomb interaction would be given by

$$V(\mathbf{q}, i\nu_m) = [V_c(q)/\kappa(q, i\nu_m)]; \\ V_c(q) \equiv (4\pi e^2/q^2), \quad \nu_m \equiv \omega_n - \omega_n' \quad (2.8)$$

where  $\kappa(q, i\nu_m)$  is the electronic dielectric function.

In the second diagram of Fig. 1, the wavy line represents the phonon propagator  $D_\lambda(\mathbf{q}, i\nu_m)$  and the right and left dots represent the electronically screened electron-phonon coupling functions,  $\tilde{g}_{\mathbf{p}, \mathbf{p}-\mathbf{q}, \lambda}(i\nu_m)$  and  $\tilde{g}_{\mathbf{p}-\mathbf{q}, \mathbf{p}, \lambda}(i\nu_m)$ , respectively. For a plane-wave approximation to the Bloch function,  $\tilde{g}$  would be a function of the momentum and energy transfer  $(\mathbf{q}, i\nu_m)$  alone and one would have

$$\tilde{g}_{\mathbf{q}\lambda}(i\nu_m) \equiv [g_{\mathbf{p}, \mathbf{p}-\mathbf{q}, \lambda}/\kappa(q, i\nu_m)]. \quad (2.9)$$

In general,  $\tilde{g}$  will depend separately upon the initial and final states,  $\mathbf{p}$  and  $\mathbf{p}-\mathbf{q}$ , of the scattered electron if crystalline anisotropy effects are important. Fortunately,  $\tilde{g}(i\nu_m)$  always enters as a factor multiplying  $D(i\nu_m)$ . Since  $D$  drops to zero as  $1/\nu_m^2$  for  $|\nu_m| > \omega_D$ , and dynamical (as opposed to static) electronic screening enters only for  $\nu_m \sim E_F \gg \omega_D$ , one can safely replace  $\tilde{g}_{\mathbf{p}\mathbf{p}'\lambda}(i\nu_m)$  by its static limit  $\tilde{g}_{\mathbf{p}\mathbf{p}'\lambda}(0) \equiv \tilde{g}_{\mathbf{p}\mathbf{p}'\lambda}$ . Furthermore, since the (longitudinal) dielectric function is essentially identical in the normal and superconducting phases,  $\tilde{g}_{\mathbf{p}\mathbf{p}'\lambda}$  can be considered to be a fixed parameter determined in the normal state.<sup>13</sup> While the long wavelength transverse dielectric function is very different in the two-phases this need not concern us since: (a) for phase space reasons only short wavelength phonons contribute appreciably to the pairing correlations; (b) shear deformation, umklapp and collision drag interactions dominate the coupling for phonons of interest to us. These interactions, however, should not be affected by the Meissner currents which modify the long wavelength transverse dielectric function in the superconducting phase. Therefore  $\tilde{g}_{\mathbf{p}\mathbf{p}'\lambda}$  is considered to be a fixed parameter which we attempt to determine from experiment. Unfortunately, first principles estimates of  $\tilde{g}$  are not fully reliable at present.<sup>14</sup>

In our approximation, phonon corrections to the electron-phonon vertex as shown in Fig. 2(a) have been neglected since they lead to corrections  $\sim (m/M)^{1/2}$  as discussed by Migdal<sup>8</sup> and Eliashberg.<sup>4</sup> The essential point is that because of the rapid decrease of  $D(i\nu_m)$

<sup>13</sup> R. E. Prange, Phys. Rev. **129**, 2495 (1963).

<sup>14</sup> Using a pseudopotential adjusted to fit high-temperature resistivity measurements, D. J. Scalapino, Y. Wada, and J. C. Swihart, Phys. Rev. Letters **14**, 502 (1964), have calculated an effective electron-phonon coupling which is in good agreement with the results reported here.

for  $|\nu_m| > \omega_D$ , only vertices in which the energy transfer  $|\omega_n - \omega_{n'}|$  is of order  $\omega_D$  or less contribute appreciably to  $\Sigma$ . For the low lying excitations of interest to us this restriction requires that  $|\omega_n|$  and  $|\omega_{n'}|$  separately be  $< \omega_D$ . It follows that the propagators of the intermediate electronic states will be small unless the Bloch energies of these states (measured relative to the Fermi surface) are also of order  $\omega_D$ . For general values of the phonon momenta  $q$  and  $q'$ , at least one of the intermediate states will be far from the Fermi surface (having an energy of order  $E_F$ ) so that a vertex correction of order  $\omega_D/E_F$  results. Physically this result corresponds to the fact that only intermediate states with particles near their mass shells contribute appreciably to  $\Sigma$ . Because of the large disparity between the speed of sound and the Fermi velocity, this restriction severely limits the phase space for virtual transitions. Only if phonons are absorbed in the inverse order to that in which they are emitted  $\mathbf{q}_1, \mathbf{q}_2, \dots, \mathbf{q}_{n-1}, \mathbf{q}_n \rightarrow \mathbf{q}_n, \mathbf{q}_{n-1}, \dots, \mathbf{q}_2, \mathbf{q}_1$  will be an appreciable contribution result, i.e., phonon line crossing graphs like that of Fig. 2(a) can be neglected.

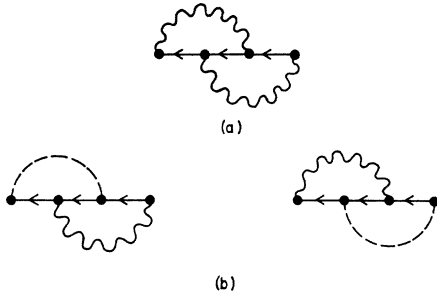


FIG. 2. Vertex corrections to the electron self-energy.

The Coulomb corrections to the electron-phonon vertex (other than screening, which has already been included) are not so simple. The lowest corrections shown in Fig. 2(b), lead to a significant change in the effective electron-phonon coupling. Fortunately, these processes lead to essentially constant scale factors multiplying  $\bar{g}_{pp'\lambda}$  of Fig 1, as Rice has shown.<sup>15</sup> Using this fact we will lump these vertex corrections in with  $\bar{g}$  to be determined from experiment. Notice that we must not include phonon corrections of the electron-Coulomb vertex if we include the corrections shown in Fig. 2(b), since this would double count graphs. Finally, there remains the Coulomb corrections to the electron-Coulomb vertex. These again lead to scale factors on the screened Coulomb interaction of Fig. 1. Since phonons are not involved here, these corrections will not give interesting energy variations of  $\Sigma$  for  $|\omega_n| < \omega_D$ , and we lump them in with the screened Coulomb interaction  $V$ .

In passing we note that in real metals, crystal momentum is conserved modulo a reciprocal lattice

<sup>15</sup> T. M. Rice (private communication).

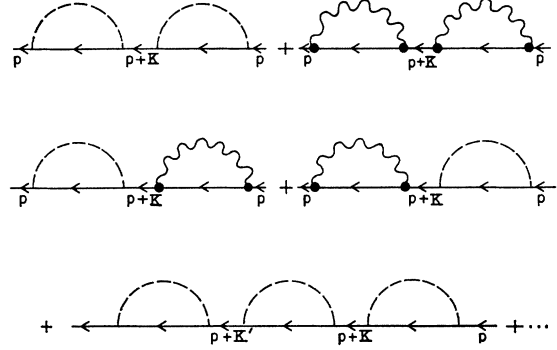


FIG. 3. Umklapp corrections to the irreducible self-energy. Here  $\mathbf{K}$  and  $\mathbf{K}'$  are reciprocal lattice vectors.

vector  $\mathbf{K}$ . Therefore, if  $\Sigma$  is defined by (2.7) (Dyson's equation) we should, strictly speaking, include self-energy graphs of the form shown in Fig. 3, where the momentum of the electron line connecting the various "irreducible" self-energy parts is *not equal* to the external electron's momentum. Since we are interested in electronic states  $\mathbf{p}$  near the Fermi surface, a state  $\mathbf{p} + \mathbf{K}$  where  $\mathbf{K}$  is a reciprocal lattice vector, will in general be far from the Fermi surface (unless  $\mathbf{p}$  happens to be very near a zone boundary). Therefore, the state  $\mathbf{p} + \mathbf{K}$  will have high excitation energy and it will in general lead to a small effect in determining the excitation spectrum except for states very near zone boundaries, which are of no special importance to us. Therefore, we neglect diagrams of the type shown in Fig. 3 in calculating  $\Sigma$ .

In view of the above discussion, the integral equation determining  $\Sigma(\mathbf{p}, i\omega_n)$  is directly obtained by writing down the contributions corresponding to the two diagrams of Fig. 1.

$$\Sigma(\mathbf{p}, i\omega_n) = -\frac{1}{\beta} \sum_{\mathbf{p}' n'} \tau_3 G(\mathbf{p}', i\omega_{n'}) \tau_3 \times \left\{ \sum_{\lambda} |\bar{g}_{pp'\lambda}|^2 D_{\lambda}(\mathbf{p} - \mathbf{p}', i\omega_n - i\omega_{n'}) + V(\mathbf{p} - \mathbf{p}') \right\}, \quad (2.10)$$

where for simplicity we have taken the screened Coulomb interaction to be a function of the momentum transfer alone. The phonon Green's function has a spectral representation of the form

$$D_{\lambda}(\mathbf{q}, i\nu_m) = \int_0^{\infty} d\nu B_{\lambda}(\mathbf{q}, \nu) \left\{ \frac{1}{i\nu_m - \nu} \right\} - \left\{ \frac{1}{i\nu_m + \nu} \right\}. \quad (2.11a)$$

Here, the spectral weight function is given by

$$B_{\lambda}(\mathbf{q}, \nu) = (1 - e^{\beta\nu} \sum_{i,j} e^{-\beta E_i} |\langle j | \varphi_{\mathbf{q}\lambda} | i \rangle|^2) \times \delta(\nu - E_j + E_i) / \sum_i e^{-\beta E_i}, \quad (2.11b)$$

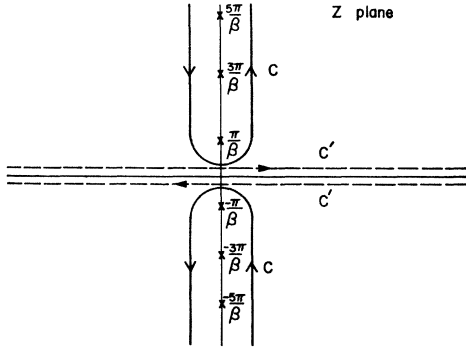


FIG. 4. Contours for changing the summation in the self-energy equation to an integration.

where

$$H|n\rangle = E_n|n\rangle. \quad (2.11c)$$

By substituting (2.11a) into (2.10) and transforming the  $n$ -summation to an integral along the contour  $c$  shown in Fig. 4, one finds

$$\begin{aligned} \Sigma(\mathbf{p}, i\omega_n) = & -\frac{1}{2\pi i} \sum_{\mathbf{p}'} \int_c dz \tau_3 G(\mathbf{p}', z) \tau_3 \\ & \times \left\{ \sum_{\lambda} \int_0^{\infty} d\nu B_{\lambda}(\mathbf{p}-\mathbf{p}', \nu) \left[ \frac{1}{i\omega_n - z - \nu} \right. \right. \\ & \times \left. \left. \frac{1}{1+e^{-\beta z}} + \frac{1}{i\omega_n - z + \nu} \frac{1}{1+e^{\beta z}} \right] \right. \\ & \left. - \frac{1}{2} V(\mathbf{p}-\mathbf{p}') \tanh(\beta z/2) \right\}. \quad (2.12) \end{aligned}$$

By deforming the contour  $c$  to  $c'$  (see Fig. 4) and using the relation

$$G(\mathbf{p}, \omega + i\delta) - G(\mathbf{p}, \omega - i\delta) = 2i \operatorname{Im} G(\mathbf{p}, \omega + i\delta), \quad (2.13)$$

which follows from the spectral representation of  $G$ , one obtains

$$\begin{aligned} \Sigma(\mathbf{p}, i\omega_n) = & -\frac{1}{\pi} \sum_{\mathbf{p}'} \int_{-\infty}^{\infty} d\omega' \operatorname{Im} [\tau_3 G(\mathbf{p}', \omega') \tau_3] \\ & \times \left\{ \sum_{\lambda} |\bar{g}_{\mathbf{p}\mathbf{p}'\lambda}|^2 \int_0^{\infty} d\nu B_{\lambda}(\mathbf{p}-\mathbf{p}', \nu) \left[ \frac{1}{i\omega_n - \omega' - \nu} \right. \right. \\ & \times \left. \left. \frac{1}{1+e^{-\beta\omega'}} + \frac{1}{i\omega_n - \omega' + \nu} \frac{1}{1+e^{\beta\omega'}} \right] \right. \\ & \left. + \frac{1}{2} V(\mathbf{p}-\mathbf{p}') \tanh(\beta\omega'/2) \right\} \\ & - \sum_{\mathbf{p}'\lambda} \int_0^{\infty} d\nu \tau_3 [G(\mathbf{p}', i\omega_n + \nu) + G(\mathbf{p}', i\omega_n - \nu)] \tau_3 \\ & \times \frac{|\bar{g}_{\mathbf{p}\mathbf{p}'\lambda}|^2 B_{\lambda}(\mathbf{p}-\mathbf{p}', \nu)}{1 - e^{\beta\nu}}. \quad (2.14) \end{aligned}$$

The contribution from the circle at infinity can be shown to vanish. This expression for  $\Sigma(\mathbf{p}, i\omega_n)$  can be analytically continued with respect to  $i\omega_n$  to the real axis from the upper half-plane by replacing  $i\omega_n$  by  $\omega + i\delta$ . In this form  $\Sigma$  is a function of the continuous (real) variables  $\mathbf{p}$  and  $\omega$ . Note that (2.14) actually represents four coupled integral equations which determine the four components of the  $2 \times 2$  matrix  $\Sigma$ . It is convenient to express these components as the coefficients of the Pauli matrix representation of  $\Sigma$ :

$$\Sigma(\mathbf{p}, \omega) \equiv (1 - Z(\mathbf{p}, \omega))\omega \mathbf{1} + \Phi(\mathbf{p}, \omega)\tau_1 + \chi(\mathbf{p}, \omega)\tau_3, \quad (2.15)$$

where we have chosen phases so that the coefficient of  $\tau_2$  is zero. It follows from (2.14) that  $Z$ ,  $\Phi$  and  $\chi$  are even functions of  $\omega$ . By combining (2.15) with Dyson's equation (2.7) one finds the analytically continued one-electron Green's function is given by

$$G(\mathbf{p}, \omega) = \frac{\omega Z(\mathbf{p}, \omega)\mathbf{1} + \bar{\epsilon}(\mathbf{p}, \omega)\tau_3 + \Phi(\mathbf{p}, \omega)\tau_1}{\omega^2 Z^2(\mathbf{p}, \omega) - \bar{\epsilon}^2(\mathbf{p}, \omega) - \Phi^2(\mathbf{p}, \omega)} \Big|_{\operatorname{Im}\omega = +\delta}, \quad (2.16a)$$

where

$$\bar{\epsilon}(\mathbf{p}, \omega) = \epsilon_{\mathbf{p}} + \chi(\mathbf{p}, \omega). \quad (2.16b)$$

Thus, the calculation of  $G$  is reduced to solving three coupled equations for the functions  $Z$ ,  $\Phi$  and  $\chi$  which determine the electron self-energy. The function  $\Delta(\mathbf{p}, \omega) = \Phi(\mathbf{p}, \omega)/Z(\mathbf{p}, \omega)$  plays the role of the energy gap parameter of the pairing theory and vanishes in the normal state.

## B. Reduction of the Self-Energy Equations

To obtain explicit solutions of the integral equations one is forced to use a computer. Fortunately a number of simplifications can be made which greatly reduce the labor involved in carrying out the computation. (1) For most purposes,  $\chi$ , which arises from the Coulomb interaction, can be included as a simple scale change of  $\epsilon_{\mathbf{p}}$  which is the same in the normal and superconducting phases. Furthermore,  $\chi$  is a slowly varying function of  $\omega$  for  $\omega < 10\omega_D$  so that  $\bar{\epsilon}$  depends just upon  $\mathbf{p}$ . (2) Since  $Z$  and  $\Phi$  vary with  $\mathbf{p}$  on a scale of order  $p_F$  we can set  $|\mathbf{p}| = p_F$  except where the behavior of these functions far from the Fermi surface is important. (3) By using these simplifications, the integration over the magnitude of  $\mathbf{p}'$  (or more generally  $\epsilon_{\mathbf{p}'}$ , for an anisotropic Fermi surface) can be explicitly performed for the terms in (2.14) involving the phonon interaction. While the corresponding integration cannot be carried out for the term arising from the screened Coulomb interaction, a pseudo-potential  $U_c$  can be introduced which accounts for virtual transitions far from the Fermi surface. With the aid of  $U_c$  one can then carry out the integral over  $\epsilon_{\mathbf{p}'}$  so that one is left with two coupled equations determining  $Z$  and  $\Delta$ , which for an isotropic (dirty) superconductor are one-dimensional equations involving the frequency variable  $\omega$ . In a clean

superconductor, the anisotropic phonon density of states, electron-phonon matrix elements and Fermi surface lead to an anisotropic self-energy.<sup>16</sup> Here we treat the impure case in which these crystalline anisotropy effects are washed out by impurity scattering, and we wish to determine the spherically averaged self-energy

$$\Sigma(\mathbf{p}, \omega) = \int d\Omega_{\mathbf{p}} \Sigma(\mathbf{p}, \omega) / 4\pi.$$

For the case in which the anisotropy due to the interaction is washed out by impurity scattering, Markowitz and Kadanoff<sup>17</sup> have shown that the spherically averaged self-energy is obtained if the effective electron-electron interaction  $|\bar{g}_{\mathbf{p}\mathbf{p}'\lambda}|^2 B_\lambda(\mathbf{p}-\mathbf{p}', \nu)$  and  $V(\mathbf{p}, \mathbf{p}')$  as well as  $\Sigma(\mathbf{p}', \omega')$  which appears in  $G(\mathbf{p}', \omega')$ , Eq. (2.14), are replaced by their spherical averages. The primary purpose of this section is to reduce (2.14) to one-dimensional form.

We begin with the phonon-interaction terms of (2.14):

$$\begin{aligned} \Sigma(\mathbf{p}, \omega)^{\text{ph}} &\equiv -\frac{1}{\pi} \sum_{\mathbf{p}'\lambda} \int_{-\infty}^{\infty} d\omega' \text{Im}[\tau_3 G(\mathbf{p}', \omega') \tau_3] \\ &\times \int \frac{d\Omega_{\mathbf{p}-\mathbf{p}'}}{4\pi} |\bar{g}_{\mathbf{p}\mathbf{p}'\lambda}|^2 \int_0^{\infty} d\nu B_\nu(\mathbf{p}-\mathbf{p}', \nu) \\ &\times \left[ \frac{1}{\omega-\omega'-\nu+i\delta} \frac{1}{1+e^{-\beta\omega'}} + \frac{1}{\omega-\omega'+\nu+i\delta} \frac{1}{1+e^{\beta\omega'}} \right] \\ &- \sum_{\mathbf{p}'\lambda} \int_0^{\infty} d\nu \tau_3 [G(\mathbf{p}', \omega+\nu+i\delta) + G(\mathbf{p}', \omega-\nu+i\delta)] \\ &\times \tau_3 \int \frac{d\Omega_{\mathbf{p}-\mathbf{p}'}}{4\pi} |\bar{g}_{\mathbf{p}\mathbf{p}'\lambda}|^2 \frac{B_\lambda(\mathbf{p}-\mathbf{p}', \nu)}{1-e^{\beta\nu}}. \quad (2.17) \end{aligned}$$

The  $\omega'$  integrand of these terms decreases as  $1/\omega'$  for  $|\omega'| \gg \omega_D$  [when the contribution from  $\omega'$  and  $-\omega'$  are added]. Thus, because of the form of  $G$ , it follows that if we are interested in excitations of energy  $\omega \sim \omega_D \ll E_F$ , the major contribution to the  $\mathbf{p}'$  integral comes from states with  $|\epsilon_{\mathbf{p}'}| \sim \omega_D$ . For this reason we can replace  $\mathbf{p}'$  by  $\mathbf{p}_F$  in  $Z$  and  $\Phi$ , occurring in the integrand. The same situation holds for the last term of (2.14). Within this approximation  $\mathbf{p}$  enters the right-hand side of (2.17) only through the momentum transfer  $\mathbf{q} \equiv \mathbf{p}-\mathbf{p}'$ , since crystalline anisotropy is washed out by impurity scattering. Therefore, we transform the sum over  $\mathbf{p}'$  to an integral over  $\bar{\epsilon}_{\mathbf{p}'}$ ,  $q \equiv |\mathbf{p}-\mathbf{p}'|$  and the azimuthal

<sup>16</sup> Starting from our results for the isotropic case, the effects of the anisotropic phonon density of states and Fermi surface on the Pb gap have been calculated by A. J. Bennett (to be published).

<sup>17</sup> D. Markowitz and L. P. Kadanoff, Phys. Rev. 131, 563 (1963).

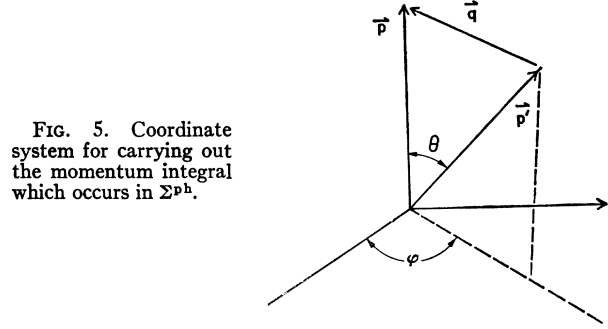


FIG. 5. Coordinate system for carrying out the momentum integral which occurs in  $\Sigma^{\text{ph}}$ .

angle  $\varphi$  as shown in Fig. 5:

$$\sum_{\mathbf{p}'} \Rightarrow \int \frac{d^3\mathbf{p}'}{(2\pi)^3} \cong \frac{m}{(2\pi)^3 \mathcal{P}_F} \int d\bar{\epsilon}_{\mathbf{p}'} q dq d\varphi, \quad (2.18a)$$

where we have defined

$$m d\bar{\epsilon}_{\mathbf{p}'} \equiv \mathbf{p}' d\mathbf{p}', \quad (2.18b)$$

and

$$\sin\theta d\theta \cong q(dq/\mathcal{P}_F). \quad (2.18c)$$

We emphasize that  $q$  is *not* restricted to the first Brillouin zone since we have formally extended the reduced-zone phonon spectrum periodically throughout  $q$  space. Thus  $\omega_{q\lambda}$  means the frequency of the phonon of mode  $\lambda$  (acoustic or optic, longitudinal or transverse) and wave vector corresponding to  $q$  reduced to the first Brillouin zone.

Since the dominant contribution to the  $\bar{\epsilon}_{\mathbf{p}'}$  integral comes from the region  $|\bar{\epsilon}_{\mathbf{p}'}| \sim \omega_D$  we extend the limits of integration of this variable to infinity and find

$$\int_{-\infty}^{\infty} d\bar{\epsilon}_{\mathbf{p}'} \tau_3 G(\mathbf{p}', \omega) \tau_3 = \{ -i\pi [\omega' Z(\omega') - \phi(\omega') \tau_1] / (\omega'^2 Z^2(\omega') - \phi^2(\omega'))^{1/2} \}, \quad (2.19a)$$

where

$$\text{Im}(\omega'^2 Z^2(\omega') - \phi^2(\omega')) > 0. \quad (2.19b)$$

On combining (2.19) and (2.16) one obtains

$$\begin{aligned} \Sigma(\mathbf{p}_F, \omega)^{\text{ph}} &= \frac{m}{(2\pi)^2 \mathcal{P}_F} \\ &\times \int_{-\infty}^{\infty} d\omega' \text{Re} \left[ \frac{\omega' Z(\omega') 1 - \phi(\omega') \tau_1}{(\omega'^2 Z^2(\omega') - \phi^2(\omega'))^{1/2}} \right] \int \frac{d\Omega_q}{4\pi} \\ &\times \int_0^{2\mathcal{P}_F} q dq \int_0^{\infty} d\nu \sum_{\lambda} B_\lambda(q, \nu) |\bar{g}_{q\lambda}|^2 \left[ \frac{1}{\omega-\omega'-\nu+i\delta} \right. \\ &\times \left. \frac{1}{1+e^{-\beta\omega'}} + \frac{1}{\omega-\omega'+\nu+i\delta} \frac{1}{1+e^{\beta\omega'}} \right] + \frac{im}{4\pi \mathcal{P}_F} \\ &\times \int_0^{2\mathcal{P}_F} q dq \int_0^{\infty} d\nu \sum_{\lambda} \sum_{s=0}^1 \left[ \frac{\omega_s Z(\omega_s) 1 - \phi(\omega_s) \tau_1}{(\omega_s^2 Z^2(\omega_s) - \phi^2(\omega_s))^{1/2}} \right] \\ &\times \int \frac{d\Omega_q}{4\pi} |\bar{g}_{q\lambda}|^2 \frac{B_\lambda(q, \nu)}{1-e^{\beta\nu}}, \quad (2.20a) \end{aligned}$$

where

$$\omega_s = \omega + (-1)^s \nu + i\delta. \quad (2.20)$$

The restriction  $q \leq 2p_F$  reflects the fact that the largest momentum transferred to a phonon occurs when an electron of momentum  $\sim \mathbf{p}_F$  scatters to a state of momentum  $\sim -\mathbf{p}_F$ .

Equation (2.20) can be simplified by transforming the negative frequency part of the  $\omega'$  integral to the positive frequency interval

$$\begin{aligned} \Sigma(\mathbf{p}_F, \omega)^{\text{ph}} &= \int_0^\infty d\omega' \operatorname{Re} \left[ \frac{\omega' Z(\omega') \mathbf{I} + \phi(\omega') \tau_1}{(\omega'^2 Z^2(\omega') - \phi^2(\omega'))^{1/2}} \right] \\ &\times (K_\pm^{\text{ph}}(\omega, \omega') f(-\omega') \mp K_\pm^{\text{ph}}(\omega, -\omega') f(\omega')) \\ &- i\pi N(0) \int_0^\infty d\nu \sum_{s=0}^1 \left[ \frac{\omega_s Z(\omega_s) \mathbf{I} - \phi(\omega_s) \tau_1}{(\omega_s^2 Z^2(\omega_s) - \phi^2(\omega_s))^{1/2}} \right] \\ &\times \sum_\lambda \int_0^{2p_F} \frac{qdq}{2p_F^2} \frac{d\Omega_q}{4\pi} |\bar{g}_{q\lambda}|^2 \frac{B_\lambda(q, \nu)}{e^{\beta\nu} - 1}. \quad (2.21) \end{aligned}$$

Here,  $\operatorname{Im}\omega' = +\delta$  and  $N(0)$  is a single-particle density of states at the Fermi surface obtained from the effective mass defined by Eq. (2.18b).

$$N(0) \equiv m p_F / 2\pi^2 \quad (2.22)$$

As we noted earlier, Eq. (2.18b) is to an excellent approximation the same in the normal and superconducting phases so that  $N(0)$  is just the density of states at the Fermi surface of the normal metal *excluding* the phonon renormalization of the electronic mass. The phonon interaction kernels  $K_\pm^{\text{ph}}$  are given by

$$\begin{aligned} K_\pm^{\text{ph}}(\omega, \omega') &= N(0) \int_0^{2p_F} \frac{qdq}{2p_F^2} \int \frac{d\Omega_q}{4\pi} \\ &\times \int_0^\infty d\nu \sum_\lambda |\bar{g}_{q\lambda}|^2 B_\lambda(q, \nu) \left[ \frac{1}{\omega' + \omega + \nu + i\delta} \right. \\ &\quad \left. \pm \frac{1}{\omega' - \omega + \nu - i\delta} \right]. \quad (2.23) \end{aligned}$$

The upper signs in (2.21) are to be used with the  $\tau_1$  matrix component and the lower signs are associated with  $\mathbf{I}$  component. The Fermi function is denoted by

$$f(\omega) = 1/(e^{\beta\omega} + 1). \quad (2.24)$$

This completes the reduction of  $\Sigma^{\text{ph}}$  to one-dimensional form.

The Coulomb part of the electronic self-energy is given by (2.14):

$$\begin{aligned} \Sigma^c(\mathbf{p}) &= - \int \frac{d^3 \mathbf{p}'}{(2\pi)^3} \int_{-\infty}^\infty \frac{d\omega'}{2\pi} \operatorname{Im}[\tau_3 G(\mathbf{p}', \omega') \tau_3] \\ &\times V(\mathbf{p}, \mathbf{p}') \tanh(\beta\omega'/2), \quad (2.25) \end{aligned}$$

where as previously discussed only the  $s$ -wave part of the Coulomb interaction  $V(\mathbf{p}, \mathbf{p}') = \int V(\mathbf{p} - \mathbf{p}') d\Omega_{\mathbf{p}-\mathbf{p}'}/4\pi$  enters in determining the  $s$ -wave part of the self-energy. Within our static screening approximation, the Coulomb contribution to  $Z(\mathbf{p}, \omega)$  vanishes, since the  $\mathbf{I}$  component of  $G(\mathbf{p}', \omega')$  is an odd function of  $\omega'$ . The Coulomb contribution to  $\chi(\mathbf{p}, \omega)$  can be neglected if the single particle energy  $\epsilon_p$  includes the static Coulomb correction to the effective mass in the normal state (which is altered by the transition to the superconducting state by a negligibly small term of order  $\Delta/E_F \sim 10^{-4}$ ). A small chemical potential shift  $\sim \Delta^2/E_F$  between the normal and super states is also neglected within this approximation. Thus we are concerned only with

$$\begin{aligned} \phi^c(\mathbf{p}) &\equiv - \frac{1}{\pi} \int_0^\infty d\omega' \int \frac{d^3 \mathbf{p}'}{(2\pi)^3} \\ &\times \operatorname{Im} \left( \frac{\phi(\mathbf{p}', \omega')}{Z^2(\mathbf{p}', \omega') \omega'^2 - \epsilon_{p'}^2 - \phi^2(\mathbf{p}', \omega') + i\delta} \right) \\ &\times V(\mathbf{p}, \mathbf{p}') \tanh(\beta\omega'/2). \quad (2.26) \end{aligned}$$

In Appendix A it is shown that the upper limit of the  $\omega'$  integration in this equation can be reduced to a cutoff  $\omega_c$  (which is conveniently chosen to be of order  $10 \omega_D$ ) providing  $V(\mathbf{p}, \mathbf{p}')$  is replaced by an energy-independent pseudopotential  $U_c$ . One is then free to perform the  $\mathbf{p}'$  integration in (2.26) by exploiting the rapid decrease of  $G(\mathbf{p}', \omega')$  for large  $|\epsilon_{p'}|$ , (so long as  $|\omega'| < \omega_c$ ). One finds

$$\begin{aligned} \phi^c(\mathbf{p}) &\cong \phi^c(\mathbf{p}_F) \\ &= -N(0) \int_0^{\omega_c} d\omega' \operatorname{Re} \left\{ \frac{\phi(\omega')}{(Z^2(\omega') \omega'^2 - \phi^2(\omega'))^{1/2}} \right\} \\ &\times U_c \tanh(\beta\omega'/2). \quad (2.27) \end{aligned}$$

The complete equation for  $\Sigma$  is given by combining (2.21) and (2.27).

### III. THE SINGLE-PARTICLE TUNNELING CURRENT

One of the initial motivations for obtaining solutions of the gap equation for a more realistic model of a metal was the structure observed in the I-V characteristics of Pb tunnel junctions.<sup>18,19</sup> This structure occurred at bias voltages of order typical phonon energies and indicated that the structure of the interaction responsible for superconductivity was experimentally observable. In this section we calculate the single-particle current flowing between a superconductor and a normal metal separated by a thin insulating barrier as a function of the applied bias voltage.

<sup>18</sup> I. Giaever, H. R. Hart, Jr., and K. Megerle, Phys. Rev. **126**, 941 (1962).

<sup>19</sup> J. M. Rowell, A. G. Chynoweth, and J. C. Phillips, Phys. Rev. Letters **9**, 59 (1962).

For the purpose of determining the single particle I-V characteristics, the tunnel junction can be described by the Hamiltonian

$$H = H_l + H_r + H_T. \quad (3.1)$$

Here  $H_l$  and  $H_r$  are the full many-body Hamiltonians for the superconductor ( $l$ ) and normal metal ( $r$ ), respectively, and  $H_T$  is the effective tunneling interaction discussed by Bardeen<sup>20</sup> and Cohen, Falicov and Phillips<sup>21</sup>

$$H_T = \sum_{\mathbf{k}l\mathbf{k}'s} (T_{\mathbf{k}l\mathbf{k}'s} c_{\mathbf{k}l s}^\dagger c_{\mathbf{k}'r s} + \text{H.c.}). \quad (3.2)$$

Here  $c_{\mathbf{k}l s}^\dagger$  creates an electron in the Bloch state ( $\mathbf{k}s$ ) in metal ( $l$ ) and  $c_{\mathbf{k}r s}$  destroys an electron ( $\mathbf{k},s$ ) in metal ( $r$ ).

As Bardeen has shown, the tunneling matrix element can be written in terms of the expectation value of the current density operator in the oxide barrier. Since the density of electrons drops to a small value in this region, an independent-particle approximation is presumed to be valid in evaluating  $T_{\mathbf{k}l\mathbf{k}'s}$ . Using Bardeen's expression, Harrison<sup>22</sup> has evaluated the tunneling matrix element within the WKB approximation and finds

$$|T_{\mathbf{k}\mathbf{k}'}|^2 = \delta_{k,|k|'} \exp \left\{ -2 \int_{x_l}^{x_r} k_\perp(x) dx \right\} / 4\pi^2 \rho_1^{(l)} \rho_1^{(r)}. \quad (3.3)$$

Here  $\rho^{(l,r)}$  are the one-dimensional density of states in metals ( $l,r$ ) for motion in the direction perpendicular to the barrier interface:

$$\rho_1 = L/\pi dk_\perp/d\xi_{k_\perp}, \quad (3.4)$$

where  $L$  is the length of the metal in the direction perpendicular to the oxide,  $k_\perp$  is the component of the wave vector perpendicular to the oxide and  $\xi_{k_\perp}$  is the energy associated with motion in this direction. Since the single-particle basis functions for the metal would be of the form

$$\varphi_k = \left( \frac{2}{L} \right)^{1/2} e^{ik_\perp x} \sin(k_\perp x + \gamma_k),$$

if one used a free-electron model, we should only consider positive values of  $k_\perp$  with a mesh of  $\pi/L$ . Since one generally performs averages over smooth, symmetric functions of  $k_\perp$ , one can alternatively include positive and negative values of  $k_\perp$  if a mesh of  $2\pi/L$  is used for  $k_\perp$ .

The delta function in (3.3) involving the components of  $k$  parallel to the barrier reflects the fact that the transmission is specular. In the exponential,  $x_l$  and  $x_r$

refer to the classical turning points, for a given energy of the tunneling particle, and a given barrier potential  $U(x)$  in the oxide layer. Here  $k_\perp(x)$  is given by

$$[2mU(x) - k_\parallel^2]^{1/2}.$$

The first term in  $H_T$  gives rise, when a bias voltage is applied, to a current flow from  $l$  to  $r$ . The transition probability per unit time for an electron to tunnel from  $l$  to  $r$  is given by

$$w_{r \leftarrow l} = 2\pi \langle \sum_F | \langle F | \sum_{\mathbf{k}l\mathbf{k}'s} T_{\mathbf{k}r\mathbf{k}l} c_{\mathbf{k}r s}^\dagger c_{\mathbf{k}l s} | I \rangle|^2 \delta(E_F - E_I) \rangle, \quad (3.5)$$

where  $F$  and  $I$  refer to the final and initial states, respectively, and the angular brackets to an ensemble average over the initial states.

In Appendix B it is shown that this expression can be reduced to

$$w_{r \leftarrow l} = \frac{A_{||} l}{16\pi^2} \int_{-\infty}^{\infty} d\omega N_{T^r}(\omega) (1 - f(\omega)) \times N_{T^l}(\omega - V) f(\omega - V). \quad (3.6)$$

Here  $A_{||}$  is the area of the barrier,  $l$  the effective square of tunneling matrix element [see Eq. (B8)], and  $f(\omega) = (e^{\beta\omega} + 1)^{-1}$  is the Fermi factor. Most important,  $N_{T^l}(\omega)$  the effective tunneling density of states, is given by

$$N_T(\omega) = \int_{-\infty}^{\infty} d\epsilon_k A(k, \omega), \quad (3.7)$$

where  $A(k, \omega)$  is the spectral weight function

$$A(k, \omega) = \frac{1}{\pi} |\text{Im} G_{11}(k, \omega)|. \quad (3.8)$$

Here  $G_{11}$  is the one-one component of the Nambu Green's function. We observe that expression for  $w_{r \leftarrow l}$  (outside of numerical factors) is just what one might write intuitively—viz., the current that flows is proportional to the product of number of electrons capable of tunneling and the number of states available to be tunneled into. However, it is not that simple. For example, at  $T=0^\circ\text{K}$ , the single-particle tunneling current arises solely from a process in which one electron from a superfluid pair in  $l$  tunnels through the barrier to a single-particle state in  $r$ . The remaining electron of the pair fills a single-particle state in  $l$ . The Fermi factors and density of states perfectly represent this case.

For temperatures greater than  $T=0^\circ\text{K}$ , the other term in  $H_T$  gives rise to a current flowing from  $r$  to  $l$  which is proportional to

$$\int_{-\infty}^{\infty} d\omega N_{T^r}(\omega) f(\omega) N_{T^l}(\omega - V) (1 - f(\omega - V)).$$

<sup>20</sup> J. Bardeen, Phys. Rev. Letters **6**, 57 (1961).

<sup>21</sup> M. H. Cohen, L. M. Falicov, and J. C. Phillips, Phys. Rev. Letters **8**, 316 (1962).

<sup>22</sup> W. A. Harrison, Phys. Rev. **123**, 85 (1961).

Thus, the tunneling current density  $j$  is given by

$$j = \frac{e}{A_{||}} (w_{r \leftarrow l} - w_{l \leftarrow r}),$$

or

$$j = \frac{et}{16\pi^2} \int_{-\infty}^{\infty} d\omega N_{T^r}(\omega) N_{T^l}(\omega - V) \times (f(\omega - V) - f(\omega)). \quad (3.9)$$

For normal metals, one can show that the tunneling density of states is just the single-particle density of states in the absence of electron-phonon interactions, since

$$\int d\epsilon_k A(k, \omega) = 1 + O\left[\left(\frac{m}{M}\right)^{1/2}\right] \quad (3.10)$$

in this case. Here  $m/M$  is the electron- to ion-mass ratio. Thus, electron-phonon interactions cancel out to order  $(m/M)^{1/2}$  in the tunneling density of states for normal metals.<sup>23</sup> Therefore, the normal-superconductor tunnel current density is given by

$$j = \frac{et}{16\pi^2} \int_0^V d\omega N_{T^r}(\omega), \quad (3.11)$$

and

$$dj/dV = [et/16\pi^2] N_{T^r}(\omega)|_{\omega=V}. \quad (3.12)$$

Thus, the differential conductance is proportional to the tunneling density of states of the superconductor.

The spectral weight function for a strong-coupling superconductor is given by

$$A(k, \omega) = \frac{1}{\pi} \left| \text{Im} \left( \frac{Z(k, \omega)\omega + \epsilon_k}{(Z^2(k, \omega)\omega^2 - \epsilon_k^2 - \varphi^2(k, \omega))} \right) \right|. \quad (3.13)$$

Since  $Z$  and  $\varphi$  are weak functions of  $k$  near the Fermi surface, the integral (3.7) for the effective tunneling density of states is simply evaluated to give

$$N_T(\omega) = \text{Re} \left\{ \frac{|\omega|}{(\omega^2 - \Delta^2(\omega))^{1/2}} \right\}. \quad (3.14)$$

This result should be contrasted with the naïve extension of the simple BCS model to allow for the energy dependence of the gap. There the spectral weight function would be written at  $T=0^\circ\text{K}$  as

$$A_{\text{BCS}}(k, \omega) = \frac{1}{2} (1 + \epsilon_k/E_k) \delta(\omega - E_k) + \frac{1}{2} (1 - \epsilon_k/E_k) \delta(\omega + E_k), \quad (3.15)$$

<sup>23</sup> This does not exclude band effects of the type reported by L. Esaki and P. J. Stiles, Phys. Rev. Letters 14, 902 (1965). Also, implicit in our neglect of vertex corrections is the assumption that the phase velocity of the phonons is small compared to that of the electrons at the Fermi surface. In semimetals and degenerately doped semiconductors this need not be the case and structure can be observed. Further, we assume the tunneling matrix elements varies on the scale of the Fermi momentum. As W. L. McMillan has pointed out, certain tunneling anomalies observed in normal metals by J. M. Rowell can be accounted for by variation of  $T_{kk'}$ , (private communication).

where  $E_k = (k^2 + \Delta^2(E_k))^{1/2}$  and hence

$$N_{\text{BCS}}(\omega) = d\epsilon_k/dE_k|_{E_k=\omega} = [\omega - \Delta d\Delta(\omega)/d\omega / (\omega^2 - \Delta^2(\omega))^{1/2}]. \quad (3.16)$$

This expression is *not* correct even when the energy variation of the gap is small and of course fails completely for those energies where the gap varies rapidly with energy and/or has a large imaginary part.

#### IV. ZERO-TEMPERATURE SOLUTIONS OF THE SELF-ENERGY EQUATIONS AND CALCULATION OF THE TUNNELING DENSITY OF STATES

Taking the zero-temperature limit of the self-energy equations (2.21) and (2.27) one finds that the energy gap  $\Delta(\omega) = \phi(\omega)/Z(\omega)$  satisfies the integral equation

$$\Delta(\omega) = \frac{1}{Z(\omega)} \int_0^{\omega_c} d\omega' \text{Re} \left\{ \frac{\Delta(\omega')}{(\omega'^2 - \Delta^2(\omega'))^{1/2}} \right\} \times [K_+(\omega', \omega) - N(0)U_c], \quad (4.1)$$

and the renormalization parameter  $Z(\omega)$  is given by

$$[1 - Z(\omega)]\omega = \int_0^{\omega_c} d\omega' \text{Re} \left\{ \frac{\omega'}{(\omega'^2 - \Delta^2(\omega'))^{1/2}} \right\} K_-(\omega', \omega). \quad (4.2)$$

As discussed in Sec. II, the frequency integral over the phonon kernel in the gap equation can be cut off at  $\omega_c \sim 10\omega_D$  because of the rapid convergence of that part of the integrand. With the introduction of the Coulomb pseudopotential  $U_c$ , the entire integral can be cutoff at  $\omega_c$ . From a computational point of view, the choice of  $\Delta(\omega)$  instead of  $\phi(\omega)$  is very useful since  $Z$  is given by a quadrature once  $\Delta$  is determined.

In order to clarify the important physical features which determine the structure of the self-energy, it is useful to write the kernels  $K_{\pm}(\omega, \omega')$  in the form

$$K_{\pm}(\omega, \omega') = \sum_{\lambda} \int_0^{\infty} d\nu \alpha_{\lambda}^2(\nu) F_{\lambda}(\nu) \left[ \frac{1}{\omega' + \omega + \nu + i\delta} \pm \frac{1}{\omega' - \omega + \nu - i\delta} \right]. \quad (4.3)$$

Here  $F_{\lambda}(\nu)$  is the phonon density of states for the  $\lambda$  mode,

$$F_{\lambda}(\nu) = \int \frac{d^3q}{(2\pi)^3} B_{\lambda}(q, \nu), \quad (4.4)$$

and  $\alpha_{\lambda}^2(\nu)$  is an effective electron-phonon coupling constant defined by

$$F_{\lambda}(\nu) \alpha_{\lambda}^2(\nu) = \frac{N(0)}{8\pi^2 v_F^2} \int d\Omega_q \int_0^{2v_F} q dq |\bar{g}_{q\lambda}|^2 B_{\lambda}(q, \nu). \quad (4.5)$$

This represents an average of the electron ( $\lambda$  mode)

phonon matrix elements over the allowed momentum transfers. The properties of the physical system which are important in determining the electron self-energy in a region of order  $\omega_c$  about the Fermi surface are contained in  $\alpha_\lambda^2(\nu)$ ,  $F_\lambda(\nu)$  and  $N(0) U_c$ . Once these are given the structure of  $Z(\omega)$  and  $\Delta(\omega)$  can be determined by solving Eqs. (4.1) and (4.2).

Data from inelastic neutron scattering<sup>24</sup> can be used to determine the phonon density of state  $\sum_\lambda F_\lambda(\nu)$ ; and, as we will see below, the I-V characteristics of superconducting tunnel junctions provide information on  $\sum_\lambda \alpha_\lambda^2(\omega) F_\lambda(\omega)$ . For Pb we estimated that the phonon density of states would have peaks near 4.4 and 8.5 (meV) of width 0.75 and 0.5 meV, respectively. In our original calculations<sup>11</sup> these peaks were represented by Lorentzians which were chosen because the integrals giving  $K_\pm$  could then be carried out analytically. However, the choice of a Lorentzian gave rise to a small but finite nonphysical phonon density of states at negative frequencies. The effects of this were minor, but could be observed in the failure of the imaginary part of  $\Delta(\omega)$  to vanish properly as  $\omega$  approached the gap edge  $\Delta_0$ . To avoid this difficulty, it is convenient to represent the phonon density of states by cut-off Lorentzians<sup>25</sup>:

$$F_\lambda(\omega) = \begin{cases} A_\lambda \left[ \frac{1}{(\omega - \omega_1^\lambda)^2 + (\omega_2^\lambda)^2} - \frac{1}{(\omega_3^\lambda)^2 + (\omega_2^\lambda)^2} \right]; & |\omega - \omega_1^\lambda| < \omega_3^\lambda \\ 0; & |\omega - \omega_1^\lambda| > \omega_3^\lambda. \end{cases} \quad (4.6)$$

Here  $A_\lambda$  normalizes  $F_\lambda(\omega)$  to unity and  $\omega_3^\lambda$  is taken as  $2\omega_2^\lambda$ . Calling the lower peak the transverse peak and denoting its values by  $\lambda = t$ :  $\omega_1^t = 4.4$  meV and  $\omega_2^t = 0.75$  meV. In the same way the upper peak will be designated as the longitudinal phonon peak with  $\lambda = l$  and  $\omega_1^l = 8.5$  meV,  $\omega_2^l = 0.5$  meV. A plot of the resulting phonon density of states

$$F(\omega) = 2F_t(\omega) + F_l(\omega) \quad (4.7)$$

in which two effective transverse polarization modes have been taken and each  $F_\lambda(\omega)$  is normalized to unity is shown in Fig. 6.

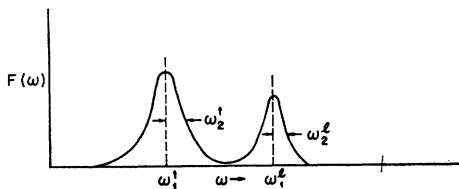


FIG. 6. Model for the lead phonon density of states  $F(\omega)$ . Here  $\omega_1^t = 4.4$  meV (milli-electron volts),  $\omega_2^t = 0.75$  meV,  $\omega_1^l = 8.5$  meV, and  $\omega_2^l = 0.5$  meV.

<sup>24</sup> B. N. Brockhouse, T. Arase, G. Caglioti, K. R. Rao, and A. D. B. Woods, Phys. Rev. **128**, 1099 (1962).

<sup>25</sup> D. J. Scalapino, Y. Wada, and J. C. Swihart, Phys. Rev. Letters **14**, 502 (1964). J. C. Swihart, D. J. Scalapino, and Y. Wada, *ibid.* **14**, 106 (1965).

It is perhaps of interest to note that these estimates of  $F_\lambda(\omega)$  were made before a full understanding of the electron tunneling data and its implication about  $\sum_\lambda \alpha_\lambda(\omega) F_\lambda(\omega)$  were known; and they were regarded as only a rough guess. Recent work by Rowell and McMillan<sup>26</sup> in which the tunneling data were used to extract  $\alpha^2(\omega) F(\omega)$ , and calculations of  $F(\omega)$  by Bennett<sup>16</sup> using the phonon dispersion relations obtained from the neutron scattering data<sup>24</sup> show that this estimate is in fact surprisingly realistic.

To complete the specifications, the behavior of the electron-phonon coupling strengths  $\alpha_\lambda^2(\omega)$  and the value of the Coulomb pseudopotential  $U_c$  must be specified. Since the peaks in the phonon density of states are relatively narrow, the frequency-dependent phonon-coupling strengths were approximated by their values at the peaks  $\omega_1^\lambda$  [i.e.,  $\alpha_t(\omega) \approx \alpha_t(\omega_1^t)$  and  $\alpha_l(\omega) \approx \alpha_l(\omega_1^l)$ ]. The strength of the longitudinal electron-phonon coupling  $\alpha_l^2(\omega_1^l) \equiv \alpha^2$  was adjusted so that the calculated value of the gap at the gap edge  $\Delta_0 \equiv \Delta(\Delta_0)$  agreed with the experimental value of 1.34 meV for ratios  $\alpha_l^2/\alpha_t^2$  of 1 and 0.5. We estimated that  $U_c = 0.11$ , and computations were carried out for  $U_c$  values of 0.11 and 0.

Before discussing the solutions of the gap equation and the resulting effective tunneling density of states for this model of Pb, it is useful to briefly consider the nature of the results for a simpler model in which the phonon density of states has just one peak, see Fig. 7(a). In the absence of  $U_c$ , the solution of the gap

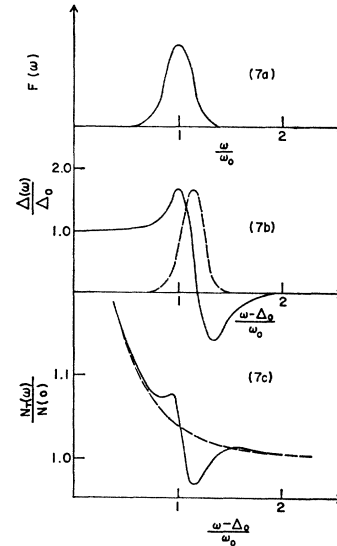


FIG. 7. Single phonon peak model as an illustration of the manner in which structure in the phonon density of states is reflected in the gap and the effective tunneling density of states. The phonon density of states  $F(\omega)$  is plotted in 7(a); the real (solid) and imaginary (dashed) parts of the gap  $\Delta(\omega)$  in 7(b); and the normalized tunneling density of states  $N_T(\omega)/N(0)$  (solid) compared with the BCS form (dashed) in 7(c).

<sup>26</sup> W. L. McMillan and J. M. Rowell, Phys. Rev. Letters **14**, 108 (1965).

Eq. (4.1) has the form shown in Fig. 7(b). Here for our present discussion we have simplified the form of these solutions by neglecting the weak structure at  $n\omega_0 + \Delta_0$  which is associated with the nonlinear nature of the gap equation. As the frequency approaches  $\omega_0 + \Delta_0$ , the real part of the gap increases and reaches a maximum at  $\omega_0 + \Delta_0$ . It then decreases, becomes negative and finally goes to zero. The imaginary part of the gap exhibits a peak slightly beyond  $\omega_0 + \Delta_0$ . This is a direct reflection of the structure of the effective electron-electron interaction. At frequencies  $\omega$  below  $\omega_0 + \Delta_0$  the bulk of the phonons which can be exchanged have frequencies greater than  $\omega$  and the effective electron-electron interaction is attractive. Physically, charge fluctuations at  $\omega < \omega_0 + \Delta_0$  are over screened by the ion-cores since the typical lattice vibrational frequencies occur at higher frequencies. When  $\omega$  is larger than  $\omega_0 + \Delta_0$ , the bulk of the phonon modes occur at lower frequencies and the ion-cores respond out of phase to  $\omega$  charge fluctuations producing a repulsive effective electron-electron interaction. This is responsible for the change in sign of the real part of  $\Delta$  at frequencies somewhat above  $\omega_0 + \Delta_0$ . In the neighborhood of  $\omega_0 + \Delta_0$ , the real part of the gap peaks because of the near resonant exchange of large numbers of phonons which enhance the electron-pair binding energy. The imaginary part of the gap also reflects this resonant exchange of phonons which becomes a maximum at frequencies  $\omega$  in the neighborhood of  $\omega_0 + \Delta_0$ .

In Fig. 7(c), the ratio of the effective tunneling density of states in the superconducting and normal states is plotted for this single-phonon peak model. To see how the structure in  $\Delta$  modifies this ratio it is useful to expand  $N_T(\omega)/N(0)$  in powers of  $\Delta/\omega$ .

$$N_T(\omega)/N(0) \approx 1 + \frac{1}{2}((\Delta_1(\omega)/\omega)^2 - (\Delta_2(\omega)/\omega)^2). \quad (4.8)$$

As  $\Delta_1$  increases above  $\Delta_0$  the effective tunneling density

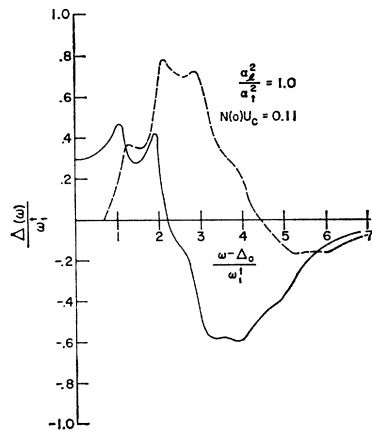


FIG. 8. Plot of the real (solid) and imaginary (dashed) parts of  $\Delta(\omega)/\omega_1^t$  versus  $(\omega - \Delta_0)/\omega_1^t$  for the model of the Pb phonon density of states Eq. (4.7). Here  $\omega_1^t = 4.4$  meV,  $\Delta_0 = 1.34$  meV,  $\alpha_t^2 = 1.2$ ,  $\alpha_t^2/\alpha^2 = 1.0$ , and  $N(0)U_c = 0.11$ .

of states increases above the BCS value (the dashed curve). This is the situation just below  $\omega_0 + \Delta_0$ . However as the phonons at the peak in the phonon-density of states can be resonantly transferred, the imaginary part of the gap rises and the effective tunneling density of states decreases. Moreover, since just above  $\omega_0 + \Delta_0$ ,  $\Delta_1$  is decreasing while  $\Delta_2$  is increasing to its peak value, this decrease in  $N_s(\omega)/N(0)$  is sharp and the curve drops below the BCS value and, in fact, can drop below unity.

In Figs. 8 and 9 results of a numerical solution of Eqs. (4.1) and (4.2) for the gap  $\Delta(\omega)$  and renormalization parameter  $Z(\omega)$  are given. These solutions are for a ratio of coupling constants  $\alpha_t^2/\alpha^2$  of 1 and a Coulomb pseudopotential  $N(0)U_c$  of 0.11. The value of  $\alpha_t^2$  necessary in order that  $\Delta_1(\Delta_0)$  equal the experimentally measured<sup>27</sup> lead gap of 1.34 meV was 1.2. The peaks in  $\Delta_1$  (solid line Fig. 8) which occur for  $(\omega - \Delta_0)/\omega_1^t$  values near 1 and 2 reflect the two peaks in the phonon density of states. Beyond the second peak, the real part of the gap decreases and becomes negative since the bulk of all the phonons occur at lower frequencies. In the present case, the real part of  $\Delta$  remains negative, asymptotically approaching a value proportional to  $U_c$ . The additional structure at  $n\omega_1^t + m\omega_1^t + \Delta_0$  ( $n$  and  $m$  integers) is associated with multiphonon processes and arises mathematically the nonlinear nature of the gap equation. In Fig. 9, a plot of the real and imaginary parts of the renormalization parameter  $Z$  are given. The structure of the effective electron-electron interaction and the underlying form of the phonon density of states is clearly reflected in  $Z$ . Asymptotically it can be seen from Eq. (4.2) that  $Z_1$  must approach unity from above. In some of the early numerical work this asymptotic behavior was violated because the integration in the  $Z$  equation was cutoff at  $\omega_c$ . This unsatisfactory feature can be simply eliminated by adding on to the numerical

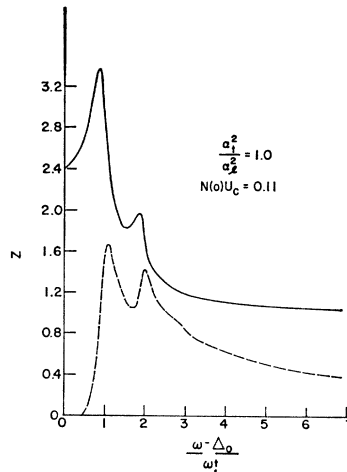


FIG. 9. Plot of the real (solid) and imaginary (dashed) parts of the renormalization parameter  $Z(\omega)$  versus  $(\omega - \Delta_0)/\omega_1^t$  for the model parameters given in Fig. 8.

<sup>27</sup> J. M. Rowell, P. W. Anderson, and D. E. Thomas, Phys. Rev. Letters 10, 334 (1963).

result obtained for the  $Z$  from (4.2) the remainder  $R(\omega)$

$$\int_{\omega_c}^{\infty} d\omega' \operatorname{Re} \left( \frac{\omega'}{(\omega'^2 - \Delta^2(\omega'))^{1/2}} \right) K_-(\omega, \omega')$$

$$\cong \int_{\omega_c}^{\infty} d\omega' K_-(\omega, \omega')$$

$$= -\frac{\alpha_t^2}{\omega} \left\{ \ln \left[ \frac{(\omega + \omega_1^t + \omega_c)^2 + (\omega_2^t)^2}{(\omega - \omega_1^t - \omega_c)^2 + (\omega_2^t)^2} \right] \right.$$

$$\left. + \frac{\alpha_t^2}{2\alpha_l^2} \ln \left[ \frac{(\omega + \omega_1^t + \omega_c)^2 + (\omega_2^t)^2}{(\omega - \omega_1^t - \omega_c)^2 + (\omega_2^t)^2} \right] \right\}. \quad (4.9)$$

The approximation is excellent since  $(\Delta(\omega_c/\omega_c)^2 \ll 1$ .

From the plots of  $\Delta_2/\omega_1^t$  and  $Z_2$  it is clear that in the vicinity of the phonon peaks the quasiparticle approximation fails completely for lead. The widths of the spectral weight function for  $\omega \sim \omega_1^\lambda$  are comparable with their positions and in addition multiple peaks associated with phonon admixtures are present. This shows the breakdown of the quasiparticle approximation referred to in the Introduction. It does not affect our calculations since we have not used this concept (or approximation) in our work.

In Fig. 10, the ratio of effective tunneling density of states  $N_T(\omega)/N(0)$  which we calculated from  $\Delta$  is plotted as the solid curve. The short-dashed curve is the BCS constant gap prediction and the dash-dot curve is experimental tunneling data obtained by plotting the ratio of the differential conductance  $dI/dV$  in the superstate to that in the normal state as a function of the bias voltage ( $\omega = V$ ). Just as for the single peaked model (Fig. 7) previously discussed, the characteristic knees near  $(\omega - \Delta_0)/\omega_1^t$  values of 1 and 2 reflect the peaks in the phonon density of states at  $\omega_1^t$  and  $\omega_1^l$ , respectively.

In order to investigate the sensitivity of these results

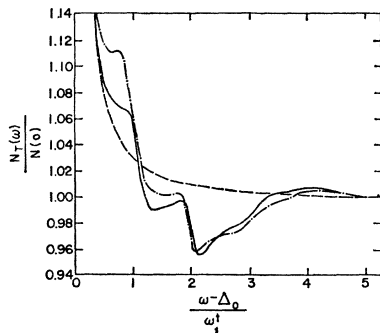


FIG. 10. The effective tunneling density of states  $N_T(\omega)/N(0) = \operatorname{Re}(\omega/(\omega^2 - \Delta^2(\omega))^{1/2})$  versus  $(\omega - \Delta_0)/\omega_1^t$  (solid) obtained from  $\Delta$  of Fig. 8. The ratio of the differential conductance of Pb in the superconducting to that in the normal state (Ref. 25) is plotted (dash-dot) as a function of  $(\omega - \Delta_0)/\omega_1^t$ . The prediction of the simplified BCS model  $\omega/(\omega^2 - \Delta_0^2)^{1/2}$  is shown as the short dashed curve.

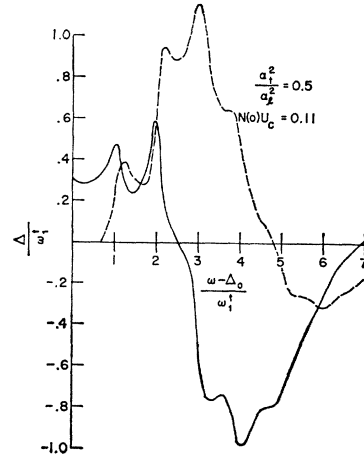


FIG. 11. Plot of the real (solid) and imaginary (dashed) parts of  $\Delta(\omega)/\omega_1^t$  versus  $(\omega - \Delta_0)/\omega_1^t$  for the model of the Pb phonon density of states Eq. (4.7). Here  $\omega_1^t = 4.4$  meV,  $\Delta_0 = 1.34$  meV,  $\alpha_l^2 = 1.6$ ,  $\alpha_l^2/\alpha_t^2 = 0.5$  and  $N(0)U_c = 0.11$ .

upon the parameters of the model the gap equation was solved for the case in which the ratio of the relative electron-phonon coupling  $\alpha_l^2/\alpha_t^2$  was reduced to 0.5. Since the size of the coupling  $\alpha_l^2$  was set by fitting  $\Delta_1(\Delta_0)$  to the experimentally determined value of 1.34 meV, the effect of reducing the  $\alpha_l^2/\alpha_t^2$  ratio is to place more weight in the longitudinal peak at  $\omega_1^l$ . This is clearly visible in the behavior of the gap, Fig. 11. The second peak in  $\Delta_1$  associated with  $\omega_1^l$  is now considerably larger than the first peak associated with the transverse phonons at  $\omega_1^t$ . This behavior is reflected in the associated tunneling density of states Fig. 12 by the large knee near  $\omega = \omega_1^l + \Delta_0$ . The strong oscillation between 2 and 3 is also a higher order manifestation of the increased strength of the longitudinal coupling. The experimental tunneling data (dash-dot) Fig. 10

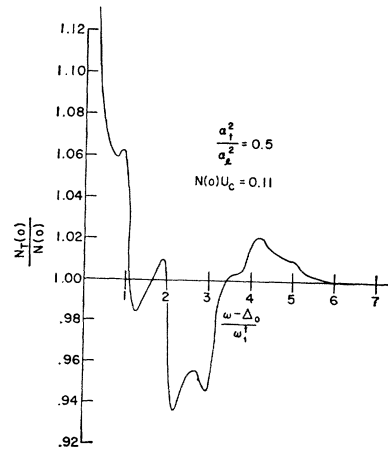


FIG. 12. The effective tunneling density of states  $N_T(\omega)/N(0) = \operatorname{Re}(\omega/(\omega^2 - \Delta^2(\omega))^{1/2})$  versus  $(\omega - \Delta_0)/\omega_1^t$  for  $\Delta$  obtained from Fig. 11. Comparison with Fig. 10 shows the increase in the size of the structure near  $\omega_1^l + \Delta_0$  which arises from the choice of  $\alpha_l^2/\alpha_t^2 = 0.5$  instead of 1.0.

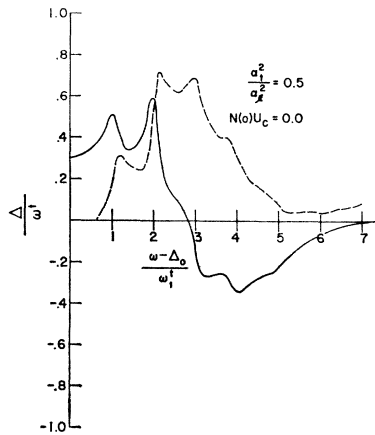


FIG. 13. Plot of the real (solid) and imaginary (dashed) parts of  $\Delta(\omega)/\omega_1^t$  versus  $(\omega - \Delta_0)/\omega_1^t$  for the model of the Pb phonon density of states Eq. (4.7). Here  $\omega_1^t = 4.4$  meV,  $\Delta_0 = 1.34$  meV,  $\alpha_r^2 = 1.3$ ,  $\alpha_l^2/\alpha_r^2 = 0.5$ , and  $N(0)U_c = 0$ .

does not exhibit this additional structure so that it is possible to distinguish quantitatively between these two different forms for  $\sum_\lambda \alpha_\lambda^2(\omega)F_\lambda(\omega)$ .

The effect of removing the Coulomb pseudopotential is shown in the behavior of  $\Delta$  plotted in Fig. 13. The ratio of the electron-phonon coupling constants  $\alpha_l^2/\alpha_r^2$  is again taken to be 0.5, and the structure of  $\Delta$  in Fig. 13 should be compared with  $\Delta$  in Fig. 11. Without the pseudopotential, the size of the electron-phonon coupling which is necessary to obtain  $\Delta_1(\Delta_0) = 1.34$  meV is reduced. This decreases the variations in  $\Delta$  and therefore ultimately reduces the structure in  $N_s(\omega)/N(0)$ . This is shown in Fig. 14 where the tunneling density of states for  $\alpha_l^2/\alpha_r^2 = 0.5$  and  $U_c = 0$  is plotted. A comparison of this case with the  $\alpha_l^2/\alpha_r^2 = 0.5$ ,  $U_c = 0.11$  case, Fig. 12, clearly shows that  $U_c$  enhances the structure in the effective tunneling density of states.

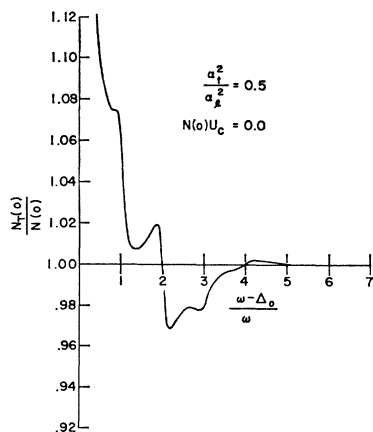


FIG. 14. The effective tunneling density of states  $N_T(\omega)/N(0) = \text{Re}[\omega/(\omega^2 - \Delta^2(\omega))^{1/2}]$  versus  $(\omega - \Delta_0)/\omega_1^t$  for  $\Delta$  obtained from Fig. 13. Comparison with Fig. 12 shows that  $U_c$  enhances the structure in the effective tunneling density of states.

## V. CONCLUSION

A conclusion to this paper seems particularly in order since the bulk of this work was completed several years ago and many of the conclusions have in fact been verified in great detail. The first and perhaps the most basic conclusion is that experimental data support the Eliashberg<sup>4</sup> form of the interaction kernel in the gap equation. They do not support the form suggested by the work of Fröhlich<sup>5</sup> or Bardeen and Pines.<sup>6</sup> These latter two interactions agree with Eliashberg's only in the static limit; however, the structure in the gap function arises from the dynamic behavior of the interaction.

This work provides a good illustration of the usefulness of Green's-function methods in solid-state problems. Here these methods provide a framework within which the retarded nature of the electron-phonon interaction and the breakdown of the quasiparticle approximation (because of the large damping at energies associated with the peaks in the phonon density of states) can be simply dealt with. For example, because of the separation of frequency and momentum variables, it is clear that the effective tunneling density of states is  $N(0) \text{Re} \omega / [\omega^2 - \Delta^2(\omega)]^{1/2}$  rather than involving derivatives of  $\Delta(\omega)$ , as a naïve quasiparticle approximation would give.

A second conclusion is that tunneling data provide a direct probe of the electron-ion system capable of measuring  $\sum_\lambda \alpha_\lambda^2(\omega)F_\lambda(\omega)$  and the Coulomb pseudopotential  $U_c$ . The sensitivity of the results for different choices of these parameters supported the choice of  $F_\lambda(\omega)$  given by Eq. (4.7) with  $\alpha_l^2/\alpha_r^2 = 1$  and  $U_c = 0.11$ . The calculated value of  $\alpha_r^2 = 1.2$  is an important measure of the effective electron-phonon strength in Pb.

Subsequently to the above work, a number of applications of the theory have been made. One of the first of these was that not only is the gross structure of the phonon density-of-states peaks observable in the I-V characteristics, but the Van Hove critical points are reflected as log and square-root singularities in  $d^2I/dV^2$  vs  $V$ .<sup>28</sup> McMillan and Rowell<sup>26</sup> have since obtained the complete  $\alpha^2(\omega)F(\omega)$  curve and  $U_c$  for Pb by a beautiful calculation in which the tunneling data are used as the input and the equations solved for the parameters of the system. These results are in remarkably close agreement with the set of parameters (see Fig. 8) for the simple model of Pb which we discussed.

In addition, the finite temperature equations have been solved for Pb using this model. Swihart, Wada and one of the authors<sup>25</sup> have found that both the anomalous  $2\Delta_0/kT_c$  ratio and critical magnetic field versus  $T$  behavior for this model are in good agreement with experiment. It is also worth noting that the imaginary part of  $\Delta$  has been used by Fibish<sup>29</sup> to explain

<sup>28</sup> D. J. Scalapino and P. W. Anderson, Phys. Rev. **133**, A921 (1964). D. J. Scalapino, Rev. Mod. Phys. **36**, 205 (1964).

<sup>29</sup> M. Fibich, Phys. Rev. Letters **14**, 561 (E) (1965); **14**, 621 (E) (1965).

the damping of the log singularity in the ratio of normal to superconducting nuclear spin-lattice relaxation time at  $T_c$ . In addition, the agreement between theory and experiment for the temperature dependence of the phonon-limited electronic thermal conductivity of strong-coupling materials is greatly improved by the above type theory, as Ambegoakar and Tewordt have shown.<sup>30</sup>

Thus, it appears that the theory of strong-coupling superconductors can account in detail for most of the discrepancies between the weak-coupling theory and experiments on strong-coupling superconductors.

### ACKNOWLEDGMENTS

The authors have benefited greatly from discussions with many people, particularly P. W. Anderson, L. P. Kadanoff, W. L. McMillan, J. M. Rowell, J. C. Swihart, and Y. Wada.

### APPENDIX A: COULOMB PSEUDO-POTENTIAL $U_c$

We derive here the Coulomb pseudopotential  $U_c$  which reduces the range of energy integration from  $0 \rightarrow \infty$  in (2.26) to  $0 \rightarrow \omega_c \sim 10\omega_D$  in (2.27). We write (2.26) in the form

$$\begin{aligned} \phi^c(\mathbf{p}) = & \frac{1}{\pi} \left[ \int_0^{\omega_c} d\omega' + \int_{\omega_c}^{\infty} d\omega' \right] \\ & \times \int \frac{d^3 \mathbf{p}'}{(2\pi)^3} \operatorname{Im} \left( \frac{\phi(\mathbf{p}', \omega')}{Z^2(\mathbf{p}', \omega')\omega'^2 - \epsilon_{\mathbf{p}', 2} - \phi^2(\mathbf{p}', \omega')} \right) \\ & \times V(\mathbf{p}, \mathbf{p}') \tanh(\beta\omega'/2). \quad (\text{A1}) \end{aligned}$$

Now  $Z(\mathbf{p}, \omega) \rightarrow 1$  and  $\phi(\mathbf{p}, \omega) \rightarrow \phi^c(\mathbf{p})$  for  $\omega \gg \omega_D$ , since the phonon-electron interaction is ineffective except for energies  $\omega > \omega_D$ . Furthermore  $\beta\omega_c \gg 1$  for temperatures at which the material is superconducting, so that  $\tanh(\beta\omega'/2) \sim 1$  for  $\omega' > \omega_c$ . Therefore the integral from  $\omega_c$  to  $\infty$  can be simplified by replacing  $Z(\mathbf{p}', \omega')$  and  $\tanh(\beta\omega'/2)$  by unity, and  $\phi(\mathbf{p}', \omega')$  by  $\phi^c(\mathbf{p}')$ , so that (A1) reduces to

$$\begin{aligned} \phi^c(\mathbf{p}) + \int \frac{d^3 \mathbf{p}'}{(2\pi)^3} V(\mathbf{p}, \mathbf{p}') \frac{\theta(E_{\mathbf{p}'} - \omega_c)}{2E_{\mathbf{p}'}} \phi^c(\mathbf{p}') \\ = \int \frac{d^3 \mathbf{p}'}{(2\pi)^3} V(\mathbf{p}, \mathbf{p}') \int_0^{\omega_c} \frac{d\omega'}{\pi} \\ \times \operatorname{Im} \left( \frac{\phi(\mathbf{p}', \omega')}{Z^2(\mathbf{p}', \omega')\omega'^2 - \epsilon_{\mathbf{p}', 2} - \phi^2(\mathbf{p}', \omega')} \right) \\ \times \tanh(\beta\omega'/2). \quad (\text{A2}) \end{aligned}$$

In the reduction we have used the relation

$$\int_{\omega_c}^{\infty} \frac{d\omega'}{\pi} \operatorname{Im} \left( \frac{1}{\omega'^2 - E_{\mathbf{p}'}^2 + i\delta} \right) = \frac{\theta(E_{\mathbf{p}'} - \omega_c)}{2E_{\mathbf{p}'}} \quad (\text{A3})$$

where

$$\theta(x) = \begin{cases} 1, & x > 0, \\ 0, & x < 0. \end{cases}$$

If we view the momentum indices  $\mathbf{p}$  and  $\mathbf{p}'$  as matrix indices and the summation over the index  $\mathbf{p}'$  as

$$\int \frac{d^3 \mathbf{p}'}{(2\pi)^3},$$

then (A2) takes the matrix form

$$(1 + \Omega)\phi^c = VF, \quad (\text{A4})$$

where the matrix elements of  $\Omega$  are given by

$$\Omega_{\mathbf{p}\mathbf{p}'} = [\theta(E_{\mathbf{p}'} - \omega_c)/2E_{\mathbf{p}'}] V(\mathbf{p} - \mathbf{p}'), \quad (\text{A5})$$

and

$$\begin{aligned} F_{\mathbf{p}'} = \int_0^{\omega_c} \frac{d\omega'}{\pi} \operatorname{Im} \left( \frac{\phi(\mathbf{p}', \omega')}{Z^2(\mathbf{p}', \omega')\omega'^2 - \epsilon_{\mathbf{p}', 2} - \phi^2(\mathbf{p}', \omega')} \right) \\ \times \tanh(\beta\omega'/2). \quad (\text{A6}) \end{aligned}$$

Since  $V$  is a repulsive potential,  $1 + \Omega$  is a nonsingular operator and (A4) can be written as

$$\phi^c = (1 + \Omega)^{-1} VF \equiv U_c F, \quad (\text{A7})$$

where the Coulomb pseudopotential  $U_c$  satisfies

$$(1 + \Omega)U_c = V; \quad (\text{A8})$$

or in component form, one has the integral equation

$$\begin{aligned} U_c(\mathbf{p}, \mathbf{p}') = V(\mathbf{p} - \mathbf{p}') - \int \frac{d^3 \mathbf{p}''}{(2\pi)^3} V(\mathbf{p}, \mathbf{p}'') \\ \times \frac{\theta(E_{\mathbf{p}''} - \omega_c)}{2E_{\mathbf{p}''}} U_c(\mathbf{p}'', \mathbf{p}'), \quad (\text{A9}) \end{aligned}$$

determining  $U_c$ . Finally, by taking components of (A7) we obtain

$$\phi^c(\mathbf{p}) = \int \frac{d^3 \mathbf{p}'}{(2\pi)^3} U_c(\mathbf{p}, \mathbf{p}') F(\mathbf{p}'). \quad (\text{A10})$$

It is clear from the form of (A6) that  $F_{\mathbf{p}'}$  decreases extremely rapidly for  $\epsilon_{\mathbf{p}'} > \omega_c$ . For this reason the major contribution to the integral in (A10) comes from states  $\mathbf{p}'$  near the Fermi surface,  $|\mathbf{p}' - \mathbf{p}_F| \ll \mathbf{p}_F$ . Since the pseudopotential  $U_c$  has appreciable variation only on the scale of  $\mathbf{p}_F$ , as is easily seen from (A9), we can replace  $U_c(\mathbf{p}, \mathbf{p}')$  by  $U_c(\mathbf{p}, \mathbf{p}_F)$  in (A10). The  $\mathbf{p}'$  integration can then be carried out with the aid of (2.18)

<sup>30</sup> V. Ambegoakar and L. Tewordt, Phys. Rev. **134**, 805 (1964); V. Ambegoakar and J. Woo, *ibid.* **139**, A1818 (1965).

and (2.19) and one finds

$$\phi^c(\mathbf{p}) = -N(0) \int_0^{\omega_c} d\omega' \operatorname{Re} \left( \frac{\Delta(\omega')}{(\omega'^2 - \Delta^2(\omega'))^{1/2}} \right) \\ \times U_c(\mathbf{p}, \mathbf{p}_F) \tanh(\beta\omega'/2). \quad (\text{A11})$$

If we are only interested in  $\phi^c(\mathbf{p})$  for momenta  $\mathbf{p} \sim \mathbf{p}_F$ ,  $\mathbf{p}$  can be set equal to  $\mathbf{p}_F$  and one obtains (2.27), where

$$U_c \equiv U_c(\mathbf{p}_F, \mathbf{p}_F). \quad (\text{A12})$$

The integral equation (A9) which determines  $U_c$  has a direct interpretation. It simply accounts for Coulomb scatterings outside the energy band  $\pm\omega_c$  about the Fermi surface which have been excluded from the numerical integration by the introduction of  $\omega_c$  in Eq. (A11). Physically, because the Coulomb interaction is repulsive, the correlations induced by the multiple scatterings taken into account in (A9) reduce the probability that the two electrons are within the range of the screened Coulomb interaction. This has the effect of making  $U_c$  smaller than the corresponding  $s$ -wave average of the plane-wave matrix element  $V(\mathbf{p}, \mathbf{p}')$ . This reduction can be explicitly determined if we approximate  $V(\mathbf{p}, \mathbf{p}')$  by a factorizable potential

$$V(\mathbf{p}, \mathbf{p}') = V_c, \quad |\epsilon_{\mathbf{p}}| \text{ and } |\epsilon_{\mathbf{p}'}| < \omega_m, \quad (\text{A13}) \\ = 0, \quad \text{otherwise.}$$

Here  $V_c$  is the average of the Coulomb interaction over the Fermi surface and  $\omega_m$  is of order the Fermi energy  $E_F$ . Using this, the solution of (A9) is

$$U_c = V_c / [1 + N(0)V_c \ln(E_F/\omega_c)] \quad (\text{A14})$$

if the density of Bloch states is taken constant for  $|\epsilon_{\mathbf{p}}| < \omega_m$ . Using values appropriate to Pb we find  $N(0)U_c = 0.11$ .

## APPENDIX B: REDUCTION OF THE TUNNELING RATE EXPRESSION

We derive here the reduction of the general expression for the tunneling rate (3.5) to the form (3.6). We define  $|m(N)\rangle$  as an exact eigenstate of the  $N$ -particle metal in the absence of both  $H_T$  and any applied voltage  $V$ .  $E_m^N$  is the energy associated with the state  $|m(N)\rangle$ . Then the delta function conserving energy can be written

$$\delta(E_F - E_I) = \delta(E_{n_r}^{N+1} + E_{n_l}^{N-1} - V - E_{m_r}^N - E_{m_l}^N) \\ = \int_{-\infty}^{\infty} d\omega \delta(E_{n_r} - E_{m_r} - \mu_r - \omega) \\ \times \delta(E_{n_l} - E_{m_l} + \mu_l - V + \omega), \quad (\text{B1})$$

where in the last expression we have dropped the encumbering superscripts. The letters  $m$  and  $n$  will be used to denote excited states containing  $N$  and  $N \pm 1$  particles, respectively. It should be noted that an

essential experimental condition is that the two metals be in thermal equilibrium at some fixed temperature. Hence we may take  $\mu_r = \mu_l = \mu$  and may carry out the ensemble averages for the two metals, independently. Finally, we observe that terms of the form

$$|\langle n_r(N+1) | \sum_{\mathbf{k}} T_{\mathbf{k}\mathbf{k}'} c_{\mathbf{k}'}^{\dagger} | m_r(N) \rangle|^2 \quad (\text{B2})$$

can be written as

$$\sum_{\mathbf{k}} |T_{\mathbf{k}\mathbf{k}'}|^2 |\langle n_r | c_{\mathbf{k}'}^{\dagger} | m_r \rangle|^2, \quad (\text{B3})$$

since the operator  $c_{\mathbf{k}'}^{\dagger}$  selects out that subset of excitations which are characterized by the wave vector  $\mathbf{k}$ .

Then, explicitly introducing Harrison's<sup>22</sup> expression for  $T_{\mathbf{k}\mathbf{k}'}$  we can write

$$w_{r \leftarrow l} = - \frac{1}{\pi} \sum_{k_{||}} \int_{-\infty}^{\infty} d\omega \exp\left(-2 \int_{z_l}^{z_r} k_{||}(x) dx\right) \\ \times \left[ \sum_{k_{||}} \frac{1}{\rho_l^{(r)}} \sum_{m_r n_r} P_{m_r} |\langle n_r | c_{\mathbf{k}'}^{\dagger} | m_r \rangle|^2 \right. \\ \times \delta(E_{n_r} - E_{m_r} - \mu - \omega) \left. \right] \\ \times \left[ \sum_{k_{||}'} \frac{1}{\rho_l^{(l)}} \sum_{m_l n_l} P_{m_l} |\langle n_l | c_{\mathbf{k}'}^{\dagger} | m_l \rangle|^2 \right. \\ \times \delta(E_{n_l} - E_{m_l} + \mu - V + \omega) \left. \right], \quad (\text{B4})$$

where  $P_m = e^{\beta\Omega} e^{-\beta(E_m - \mu N)}$  and we have carried out the spin sum. Note that  $k_{||}$  and  $k_{||}'$  have only positive values. The sum over  $k_{||}$  can be done first. In principle, the expression in the square brackets depends on  $k_{||}$  but in practice such dependence is very weak. Furthermore, since the exponential factor decreases rapidly with increasing  $k_{||}$ , only electrons moving perpendicular to the barrier contribute significantly to the tunneling current. If we consider a wave function which is mainly in the right-hand metal with an exponentially decreasing tail in the barrier, then

$$E_{n_r} - E_{m_r} = U(x) + \left\{ \epsilon_{k_{||}} - \frac{k_{||}^2(x)}{2m} + \mu \right\}, \quad (\text{B5})$$

where  $U(x)$  is the barrier potential and

$$\epsilon_{k_{||}} + \mu = k_{||}^2/2m.$$

The use of the bare electron mass is consistent with our treatment of the barrier as a potential step (with rounded shoulders). In addition to the possibility of structure in the barrier we are also neglecting image force corrections to the barrier potential and any asymmetry in that potential due to bias voltage or to

fabrication procedures. While such effects are certainly present we do not believe their inclusion is essential to an understanding of the  $I$ - $V$  characteristics of the metal-insulator—metal tunneling processes for very small voltages. The sum over  $k_{||}$  can then be written as

$$\frac{A_{||}}{8\pi^2} \int_0^{2\pi} d\varphi \int_0^{k_c^2} dk_{||}^2 \exp \left\{ -2 \int_{x_l}^{x_r} dx \right. \\ \left. \times (2m(U(x) + E_m - E_n) + k_{||}^2)^{1/2} \right\}, \quad (\text{B6})$$

where  $A_{||}$  is the area of the barrier. We assume that  $U(x)$  changes rapidly (but not so rapidly that the WKB approximation is invalid) in the vicinity of  $x_r$  and  $x_l$  so that for most of the barrier region  $U(x) = U_{\max}$ . We define the metal-barrier work function  $\varphi = U_{\max} - \mu$ . A precise specification of the cutoff  $k_c^2$  of the  $k_{||}^2$ -integral is immaterial since only the region around  $k_{||} \sim 0$  is important. For small applied voltages and at low temperatures only states near the chemical potential will contribute to the tunneling current. So in the case where  $V \ll \varphi$ , the integral (B6) over  $k_{||}$  is well represented by

$$A_{||}t/4\pi, \quad (\text{B7})$$

where

$$t = 1/d((2m\varphi)^{1/2} + 1/2d) \exp(-2d(2m\varphi)^{1/2}), \quad (\text{B8})$$

and  $d \approx x_r - x_l =$  barrier thickness.

Now we consider the expressions in the square brackets in (B4) and their relation to the one-particle Green's functions. An alternative way of writing the one-one component of the Green's function defined by Eq. (2.3a) in Sec. II is

$$G_{11}(k, \tau) = -\sum_m \rho_m \langle m | T c_k(\tau) c_k^\dagger(0) | m \rangle. \quad (\text{B9})$$

Then by inserting a complete set of states one can easily show that

$$\sum_{m,n} \rho_m |\langle n | c_k^\dagger | m \rangle|^2 \delta(E_n - E_m - \mu - \omega) \\ = A(k, \omega)(1 - f(\omega)), \quad (\text{B10})$$

and

$$\sum_{m,n} \rho_m |\langle n | c_k | m \rangle|^2 \delta(E_n - E_m - \mu + \omega) \\ = A(k, \omega)f(\omega), \quad (\text{B11})$$

where  $f(\omega) = (1 + e^{\beta\omega})^{-1}$  and  $A(k, \omega)$  is the spectral weight function

$$A(k, \omega) = -\frac{1}{\pi} \text{Im} G_{11}(k, \omega + i\delta). \quad (\text{B12})$$

While a portion of the temperature dependence has been accounted for by the introduction of the Fermi factors,  $A(k, \omega)$  will also have temperature dependence. It is convenient to define the effective tunneling density of states by

$$N_T(\omega) = N(0) \int_{-\infty}^{\infty} d\epsilon_k A(k, \omega), \quad (\text{B13})$$

since then our final expression for the transition rate  $w_{r \leftarrow l}$  (B15) has formally the same structure as that for tunneling between two systems of noninteracting electrons where  $N_T(\omega)$  would be just  $N(0)$  near the Fermi surface.

Finally, consider the  $k_{\perp}$  sums. In the continuum approximation it is more convenient to sum over both signs of  $k_{\perp}$  (and reduce  $\rho_{\perp}$  by a factor of two). Then since  $\epsilon_{k_{\perp}}$  is not limited by any essential restrictions from  $k_{||}$  we can replace  $\epsilon_{k_{\perp}}$  by  $\epsilon_k$ . Thus, the square bracket involving the sum over  $k_{\perp}$  in (B4) becomes

$$\frac{1}{2} \int_{-\infty}^{\infty} d\epsilon_k \sum_{n_r m_r} P_{m_r} |\langle n_r | c_k^{\tau\dagger} | m_r \rangle|^2 \\ \times \delta(E_{n_r} - E_{m_r} - \mu - \omega) \\ = \frac{1}{2} N_r(\omega)(1 - f(\omega)). \quad (\text{B14})$$

In a similar manner one can reduce the second square bracket in (B4) and obtain the desired reduction of Eq. (3.5) to (3.6),

$$w_{r \leftarrow l} = \frac{A_{||}t}{16\pi^2} \int_{-\infty}^{\infty} d\omega N_T^r(\omega)(1 - f(\omega)) \\ \times N_T^l(\omega - V)f(\omega - V). \quad (\text{B15})$$